

AFIT/GAP/ENP/93D-03

②

AD-A273 727

DTIC
ELECTE
DEC 16 1993
S A

INFRARED FLUORESCENCE STUDIES OF
ELECTRONIC-TO-VIBRATIONAL ENERGY
TRANSFER IN A Br_2 :NO SYSTEM

THESIS

Michael R. Hawks
First Lieutenant, USAF
AFIT/GAP/ENP/93D-03

Approved for public release; distribution unlimited

98 12 151 27

93-30513

AFIT/GAP/ENP/93D-03

INFRARED FLUORESCENCE STUDIES OF
ELECTRONIC-TO-VIBRATIONAL ENERGY
TRANSFER IN A Br₂:NO LASER SYSTEM

THESIS

Presented to the Faculty of the Graduate School of Engineering
of the Air Force Institute of Technology

Air University

In Partial Fulfillment of the Requirements for the
Degree of Master of Science in Physics

Michael R. Hawks, P. S.
First Lieutenant, USAF

December 1993

Accession For	
NTIS CRA&I	<input checked="checked" type="checkbox"/>
DTIC TAB	<input type="checkbox"/>
Unannounced	<input type="checkbox"/>
Justification	
By	
Distribution /	
Availability Codes	
Dist	Avail and/or Special
A-1	

Approved for public release; distribution unlimited



ACKNOWLEDGMENTS

This research follows very closely from the research of Captain Ray Johnson. Much of his apparatus and many of the results of his study are used in this study. To follow his example, I shall also share a philosophical lesson that I learned from this research experience: the easy way is rarely that, because after it fails, you have to go back and do it right. Ray's hard work and his words of advice (as well as his caustic wit) are tremendously appreciated, although he might not believe it from the way his advice was sometimes taken.

Many thanks also to Major Glen Perram, the advisor/mentor for this thesis. His knowledge of the field, as well as his dedication and patience, are unsurpassed. I often wonder which of us actually worked harder on this project.

Also, to Roy Calfas, Greg Williams, and Norton Utilities; thank you for retrieving the data off of my damaged floppy disk, and thanks to MKS for making the only piece equipment in my lab that never broke. Lastly, thanks to lab technicians Greg Smith and Jim Reynolds for their support, and to Mike Ray of the Wright Labs glass shop for dealing with all of the special manufacturing requests.

Michael R. Hawks

TABLE OF CONTENTS

Acknowledgements	ii
List of Figures	v
List of Tables	vii
List of Symbols	viii
Abstract	ix
I. INTRODUCTION	1
A. Motivation	1
B. Problem Statement	5
II. THEORY	6
A. Introduction	6
B. Summary of Current Knowledge	6
C. Solution to Rate Equations	12
D. Analysis Methods	16
1. Bromine Self-Quenching Rate.	16
2. Br^* Quenching by NO.	17
3. Analysis of NO fluorescence.	18
III. EXPERIMENT	21
A. Experimental Setup	21
1. Main Apparatus.	21
2. Gas Handling System.	25
B. Experimental Procedures	26
1. Bromine Distillation.	26
2. Detector Alignment.	27
C. Experiments Performed	28
1. Br^* Lifetime.	28
2. $\text{E} \rightarrow \text{V}$ Transfer Rate.	28
3. Branching Fraction for $\text{E} \rightarrow \text{V}$ Transfer.	29
IV. RESULTS	33
A. Introduction	33
B. Quenching Rates for Br_2 and NO on Br^*	33

C. NO fluorescence Data	36
D. Conclusions	41
1. Recommendations for Future Research.	41
2. Conclusions.	42
V. BIBLIOGRAPHY	43
Appendix A: Spectroscopic Notation	45
A. Introduction	45
B. Atomic Bromine	45
C. Molecular Bromine and Photolysis	47
Appendix B: Transmission of Cold NO Filter	49
Appendix C: Fluorescence Data for NO	52
Appendix D: Analysis of Functional Form Used in Curve Fitting	57
Vita	59

LIST OF FIGURES

Fig 1: Experimental apparatus.	21
Fig 2: Measured transmittance of 5.0 micron long-pass filter used for observations of NO fluorescence.	22
Fig 3: Response curve for the InSb detector, as measured.	23
Fig 4: Apparatus used for measurement of detector response.	24
Fig 5: Gas handling system.	25
Fig 6: Comparison of amplifier response.	32
Fig 7: Bromine fluorescence as a function of bromine pressure with no NO present, corrected for absorption of the pump laser.	34
Fig 8: Stern-Volmer plot for Br* fluorescence, in the absence of NO.	35
Fig 9: Inverse Br* signal vs. NO pressure, in the presence of 2.0 Torr Br ₂ .	36
Fig 10: NO fluorescence vs NO pressure with 3.0 Torr bromine, with and without cold NO filter in place.	37
Fig 11: NO fluorescence vs. NO pressure for several different bromine pressures.	38
Fig 12: Ratio of observed intensity with the cold NO filter to observed intensity without the filter, for 3.0 Torr of Br ₂	39
Fig 13: Potential energy curves for molecular bromine.	48
Fig 14: Transmission of cold NO filter.	50

Fig 15: Detail of cold NO filter transmission (0.02 cm ⁻¹ resolution)	51
Fig 16: NO fluorescence vs. NO pressure with 500 mTorr of bromine, with and without cold filter.	52
Fig 17: NO fluorescence vs NO press with 750 mTorr of bromine, with and without cold filter.	53
Fig 18: NO fluorescence vs NO pressure for 1.0 Torr bromine, with and without cold filter.	53
Fig 19: NO fluorescence vs NO pressure for 3.0 Torr bromine, with and without cold filter.	54
Fig 20: NO fluorescence vs NO pressure with cold filter, for a family of bromine pressures	55
Fig 21: NO fluorescence vs NO pressure, viewed without cold filter, for a family of bromine pressures.	56

LIST OF TABLES

Table 1: Reported values for bromine self-quenching rate.	7
Table 2: Reported values for NO quenching rates.	8

LIST OF SYMBOLS

Br^*	Electronically excited bromine atoms ($^2\text{P}_{1/2}$ state).
$\text{NO}(n)$	Nitric oxide in the n th vibrational level.
k_{pump}	Rate constant for photolysis of Br_2 by pump laser.
$k_Q^{(\text{Br})}$	Rate constant for quenching of Br^* by molecular bromine, also called bromine self-quenching rate.
$k_Q^{(n)}$	Rate constant for quenching of the n th vibrational level of NO by collision with Br_2 .
k_n	Rate constant for collisional $\text{E} \rightarrow \text{V}$ transfer from Br^* into the n th vibrational level of NO. Total rate for quenching of Br^* by NO is ($k_1 + k_2$).
k_2/k_1	The branching ratio for $\text{E} \rightarrow \text{V}$ transfer to NO.
$k_{\text{V-V}}$	Rate constant for $\text{V} \rightarrow \text{V}$ transfer in NO.
$k_{\text{V-T}}^{(n)}$	Rate constant for $\text{V} \rightarrow \text{T}$ transfer, or quenching of NO in the n th excited state by ground state NO.
Γ_{Br}	Rate constant for radiative relaxation of Br^* and quenching by collisions with the chamber wall, etc.
Γ_n	Rate constant for radiative relaxation of the n th vibrational level of NO and quenching by collisions with the chamber wall, etc.
$[\text{A}]$	Concentration of species A.
$I(x)$	Intensity of the radiation from source x .
D_λ	Detector response at wavelength λ .
a_λ	Detector response at wavelength λ , expressed in terms of $D_{5.3}$.

ABSTRACT

Steady-state photolysis techniques were used to study electronic-to-vibrational energy transfer mechanisms from atomic bromine to nitric oxide. Molecular bromine was photodissociated by 488nm radiation to produce equal parts $\text{Br}(^2\text{P}_{1/2})$ and $\text{Br}(^2\text{P}_{3/2})$. Side fluorescence intensity from $\text{Br}(^2\text{P}_{1/2})$ at $2.7\text{ }\mu\text{m}$ and from $\text{NO}(v = 1 \text{ and } 2)$ around $5.3\text{ }\mu\text{m}$ were measured as a function of bromine pressure and nitric oxide pressure. The branching ratio for collisional transfer into the first and second excited states of NO was determined, and previously reported rates for quenching of NO by molecular bromine were verified.

INFRARED FLUORESCENCE STUDIES OF ELECTRONIC-TO-VIBRATIONAL ENERGY TRANSFER IN A Br_2 :NO SYSTEM

I. INTRODUCTION

In this experiment, steady state photolysis was used to create electronically excited atomic bromine in a mixture with nitric oxide. Electronic energy in the bromine is collisionally transferred to vibrational energy in the nitric oxide. The side fluorescence of the NO was measured with and without a cold NO filter, and the relative intensities of the vibrational transitions were compared to characterize the kinetics of energy transfer from Br^* to NO.

A. *Motivation*

The development of infrared (IR) countermeasures is of great interest to the United States Air Force. Improved protection against IR homing missiles would allow for greater survivability as well as an ability to strike against heavily defended targets. Since the detector on a heat seeking missile must obviously be very sensitive to IR radiation, a high-power IR laser could "blind" or even destroy the sensor, rendering the missile useless. In order for this to be effective, though, the laser must be able to deliver kilowatts of energy in one of

the atmospheric transmission bands (wavelengths from 3 to 5 microns or 8 to 14 microns). The wavelength of the laser must furthermore be tunable within this band to prevent the use of a simple filter in the nose of the missile to block the laser.

Possible candidates for the laser system include chemical lasers, diode lasers, photolytic lasers, and optically pumped lasers. Chemical lasers have been proven to produce large amounts of power, but are as yet much too large to put on an airframe in a tactical defense role. Diode lasers are extraordinarily small, but at this time diode lasers are not capable of producing the required power density. The remaining schemes, photolysis and optical pumping, are quite similar. In the optical pumping scheme, the pump laser directly excites the lasing species, while in the photolysis scheme, the "pump" laser photodissociates some molecule into one or more excited state atoms, which then collisionally transfer energy to the lasing species.

The key advantage to photolysis over optical pumping is that there is a relatively wide pumping band which will result in photolysis, while a very precise wavelength is required for direct excitation to a specific state. Not only does this make the system a bit more stable for operation in a high stress, high vibration environment like an airplane, but it allows us to choose from a variety of pump sources. One system that has been explored for this role is a system involving photolysis of halogens which collisionally transfer energy to some

receptor molecule. This excited molecule relaxes back to the ground state via radiation, forming the laser. The rotational distribution within the excited vibrational states provides about a micron of line-tunable range.

Bromine is especially attractive for use in this role for several reasons. First, excited atomic bromine is easily and efficiently produced by photolysis of molecular bromine by the 488 nm line of an argon-ion laser, or a number of other sources (frequency-doubled YAG on IBr, for example)⁽¹⁾. This results in nearly equal parts ground state bromine ($^2P_{3/2}$) atoms and electronically excited ($^2P_{1/2}$) atoms, henceforth referred to as Br*. Each Br* atom has an energy of 3685 cm⁻¹, placing it well within the IR regime.

Secondly, Br* has a very long radiative lifetime of 1.1 seconds⁽²⁾ compared to a collisional lifetime of a few microseconds. This means that only a small fraction of the Br* atoms will have a chance to radiate before collisionally transferring their energy. The primary mechanism for relaxation of Br* is collisional quenching, either by molecular bromine or by some other molecule.

Many molecules have been examined as possible receptor species. The primary requirements for an effective laser are rapid quenching of Br*, population inversion, and strong transitions within the atmospheric transmission windows. Ideally, the receptor should have a quenching rate on Br* higher than the Br₂ (self-quenching) rate of 1.2×10^{-12} cm³/molec-sec^(3,4).

Of the species that have been explored, only a few meet these criteria. Most notably, CO_2 and HCl have quenching rates in excess of ten times the bromine self-quenching rate.⁽³⁾ Water has had reported values for Br^* quenching rates of $5.1 \times 10^{-11} \text{ cm}^3/\text{molec-sec}^{(5)}$ and $6.2 \times 10^{-11} \text{ cm}^3/\text{molec-sec}^{(1)}$. Unfortunately, water is one of the main contributors to atmospheric absorption, making it difficult to find a transition that does not fall within an absorption band.

Other species that have reported quenching rates in excess of the bromine self-quenching rate include H_2 , D_2 , HI , HBr , HF , N_2O , and CH_4 . A study by Houston⁽¹⁾ showed that all of these, with the exception of CH_4 and HI which were not studied, would not be able to achieve the necessary inversion. This is based on measurements of the average number of vibrational quanta excited. In general, the n th energy level carries roughly n times the energy of the first state, so the spacing between states is roughly constant. A particle in the n th level therefore carries n quanta of energy, so the average number of quanta excited is another way of expressing the branching ratio. If the average number of quanta excited is one, then all of the pump energy goes into the first excited state. It is not practical to try to achieve inversion between the first excited level and the ground state. In order to have inversion between the second excited level and the first, we need a species with an average number of quanta excited greater than 1.5. Of the species listed so far, only CO_2 , H_2O and NO have sufficient quenching rates, transitions in atmospheric windows, and the possibility for

population inversion. Other species have been demonstrated to lase in the IR in an E-V pumping scheme, including HCN, C₂H₂, and N₂O. A diatomic molecule would be preferred because the partition function in a diatomic molecule does not allow as many modes, meaning more energy in each mode. All of these have been demonstrated to lase with Br*, but NO is the only diatomic molecule.

The quenching rate of NO on Br* is 2.4×10^{-12} cm³/molec-sec,⁽³⁾ which is significantly slower than the rates for CO₂ or HCl, but it is still well above the bromine self-quenching rate. The average number of quanta excited in NO is in excess of 1.5, which suggests the possibility for achieving inversion. This has been attributed to the near resonance of the second vibrational level (3724 cm⁻¹) with Br* (3685 cm⁻¹). The difference in the two energies is much less than kT at room temperature, so nearly all collisions will carry enough extra translational energy to make up for this difference and excite the v=2 state.

B. Problem Statement

Br* pumped nitric oxide lasers have been successfully demonstrated.^(6,3) In order to properly understand the lasing properties of NO, it is important to know the relative populations of each vibrational level. The goal of this research is to determine the mechanisms and rates for energy transfer in a Br₂:NO photolysis system.

II. THEORY

A. Introduction

This chapter will present the background information relevant to this study. Prior research in the area will be reviewed, followed by a discussion of the mechanism for the reaction and the resulting rate equations. A summary of the analysis methods used to determine the rate constants from the data will also be presented. The reader is also referred to Appendix A for a brief review of the spectroscopic notation pertaining to this chapter, as well as details concerning the photolysis of molecular bromine.

B. Summary of Current Knowledge

The rates for quenching of Br^* by Br_2 and by NO have been well studied. Additionally, some studies have dealt with the branching fraction for $\text{E} \rightarrow \text{V}$ transfer into the vibrational states of NO, and the $\text{V} \rightarrow \text{V}$ transfer rate of NO.

The first study of $\text{E} \rightarrow \text{V}$ transfer from excited halogens was done by Donovan and Husain⁽⁷⁾ in 1970. They reported rates for quenching of Br^* by several different molecular species. They reported a total quenching rate for NO on Br^* of $4.7 \times 10^{-11} \text{ cm}^3/\text{molec-sec}$, and proposed that this unusually high rate might be due to the paramagnetic nature of NO. They also reported a Br_2

self-quenching (deactivation of Br^* by collision with Br_2) rate of 1.9×10^{-11} $\text{cm}^3/\text{molec-sec}$.

Later studies reported much lower rates for bromine self-quenching. Leone and Wodarczyk were the next to study energy transfer from excited halogens. They found a rate of 4.8×10^{-13} $\text{cm}^3/\text{molec-sec}$ for bromine self-quenching. This is much more in line with other reported values. Table 1, from data originally compiled by Tate,⁽⁸⁾ shows all the published values for quenching of Br^* by Br_2 , and the dates of the research.

Table 1: Reported values for bromine self-quenching rate.

Self-Quenching Rate [$\times 10^{-12}$ $\text{cm}^3/\text{molec-sec}$]	Presented by	Date
19.0	Donovan and Husain ⁽⁷⁾	1970
0.48	Leone and Wodarczyk ⁽⁹⁾	1974
1.2	Hariri, Peterson, and Wittig ⁽⁴⁾	1976
0.47	Hofmann and Leone ⁽¹⁰⁾	1978
0.99	Kushawaha ⁽¹¹⁾	1979
1.20	Johnson ⁽³⁾	1992

The quenching rate for NO that was reported by Donovan and Husain was also exceptionally high compared to later values. Table 2 shows the values for quenching of Br^* by NO that have been found. The quenching rate for NO on Br^* reported in these studies is the total quenching rate, which is the sum of the rates for transfer into the individual vibrational levels.

Houston's experiment⁽¹⁾ used two different techniques to measure E→V transfer rates from excited halogens to a variety of molecules. The first method

Table 2: Reported values for NO quenching rates.

NO Quenching Rate [$\times 10^{-12}$ cm³/molec-sec]	Presented By	Date
47.0	Donovan and Husain ⁽⁷⁾	1970
2.0	Houston ⁽¹⁾	1981
5.3	Wight ⁽¹²⁾	1986
2.39	Johnson ⁽³⁾	1992

involved studying the side fluorescence, or spontaneous emission from the molecules. The second technique used stimulated emission in order to produce enough signal to use a monochromator. In both cases, both Br* and I* were studied, and the transfer rates for several different receptors were compared. Species studied as receptors included HF, HCl, HBr, H₂, H₂O, HD, D₂, NO, CO₂, N₂O, COS, CS₂, and HCN. In addition, a buffer gas was included in the cell to ensure thermal equilibrium with the wall. Noble gasses were generally chosen as buffers, due to their exceptionally low quenching rates.

In the fluorescence experiment, a frequency doubled Nd:YAG laser (530nm) was used to photodissociate Br₂ and a frequency quadrupled Nd:YAG (266nm) was used to photodissociate CF₃I. Mirrors were used to pass the pump beam through the cell several times, increasing absorption. In addition to an interference filter, a cell filled with the quenching gas in the ground state could

be placed before the detector to selectively absorb light from transitions to the ground state. The fluorescence was received by a variety of detectors, depending on the wavelength of the observed transition.

The reaction cell for the stimulated emission experiment consisted of three concentric glass cylinders. The innermost cylinder contained the halogen, the quenching gas, and the buffer gas. The outermost shell contained xenon, which was used as a flashlamp to excite a chemical dye in middle layer. The dyes were chosen to absorb the xenon flashlamp radiation and reemit between 480 and 500nm for bromine, or at 490nm to dissociate I_2 . The inner tube had Brewster windows at the ends, and was placed in an optical cavity. The halogens were excited via flash photolysis, and the energy was collisionally transferred to the upper lasing level in the quenching species. The resulting laser pulse was bright enough to resolve with a monochromator, so that the exact transition could be determined.

These are both pulsed experiments, so by examining the time resolved intensity from the quenching gas and solving the rate equations, the rise time and decay times could be used to find the quenching rate constant. Houston's measurement of the average number of quanta excited is based on spectrally resolving the stimulated emission to find the population of each excited state. Since a molecule in the n th state carries n quanta of energy, the average number of quanta excited is

$$\bar{Q} = \frac{\sum_i i N_i}{\sum_i N_i}$$

where i is the vibrational level.

Wight's experiment⁽¹²⁾ used a fluorescence technique very similar to Houston's to study the quenching rate of NO, as well as the branching fraction and the vibrational-to-vibrational (V→V) transfer rate, which represents the rate for redistribution of the vibrational energy. Wight, however, used photolysis of CF₃Br to produce Br*. This choice was driven by the suspicion that NO would react with the molecular bromine to form NOBr, which also emits near 5.4 microns. The CF₃Br was photodissociated by an ArF excimer laser operating at 193nm.

The fluorescence from the NO was observed with a HgCdTe detector with an active area of 25 mm², through an interference filter that passed both the v=2 → v=1 transition (5.41 microns) and the v=1 → v=0 transition (5.33 microns). By solving the rate equations and analyzing the NO fluorescence rise time and relaxation rate, Wight determined a quenching rate of 5.3x10⁻¹² cm³/molec-sec and a V→V transfer rate of 1.2x10⁻¹² cm³/molec-sec.

Wight also used a cold NO filter filled with 30-100 Torr of room temperature NO to absorb the radiation from the 1 to 0 transition. By comparing the fluorescence with and without NO in the filter, he determined the ratio [NO(v=2)] / [NO(v=1)] to be about 6.1.

A later study by Johnson⁽³⁾ measured the quenching rate of NO on Br* using a CW technique, resulting in a number in good agreement with Houston's value. In Johnson's experiment, an argon-ion laser operating at 488nm was used to produce Br* from Br₂. Side fluorescence of the mixture was observed on an InSb detector. Total pressure in the reaction chamber was monitored using a pressure transducer, and the bromine concentration was also measured by monitoring the absorption of 409nm light across the cell. This absorption diagnostic showed no change in bromine pressure with the addition of NO, refuting Wight's concerns about the production of NOBr.

Obviously the analysis of the rise and decay times used by both Houston and Wight cannot be used in a CW experiment, so Johnson's analysis differs slightly. By constructing a Stern-Volmer plot of intensity versus pressure and examining the slope and intercept, it is possible to find the ratios of rate constants. If one of these constants can be measured using a pulsed technique, the other values can be deduced, relative to the measured quantity. The quantity Johnson chose to measure was the self-quenching rate of bromine, which was found to be 1.2×10^{-12} cm³/molec-sec. This was done using an excimer pumped dye laser. Although the procedure sounds more involved, the amount of data that can be obtained in a short amount of time in a CW regime allowed Johnson to catalog the quenching rates of 24 other molecules. In addition to species

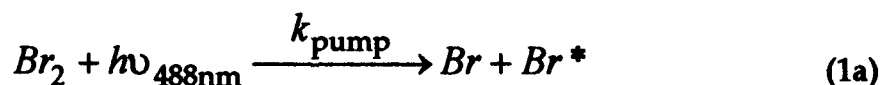
already studied by Houston, Ar, CF₄, H₄, CO, COS, H₂S, He, HI, Kr, N₂, Ne, NO₂, SF₆, SO₂, and Xe were studied.

Johnson went on to demonstrate a Br*:NO laser, using photolysis of IBr by a Nd:YAG to produce Br*. The system lased on the $v = 2 \rightarrow v = 1$ transition, proving that the rate for collisional pumping of $v = 2$ must be greater than the rate for pumping of $v = 1$. The pulse duration and the dependence of the output power on NO pressure and pump power were all characterized.

C. Solution to Rate Equations

The reaction mechanism used in this study to find branching fraction is as follows:^(3,8,13)

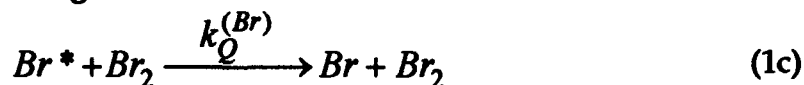
Photolysis:



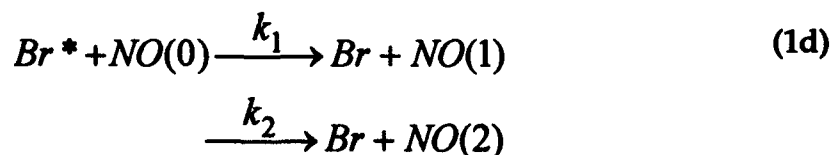
Br* radiative decay:



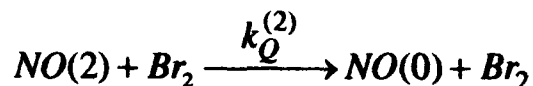
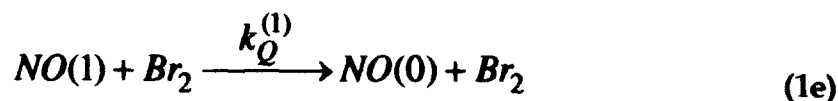
Bromine self-quenching:



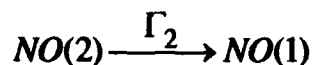
E→V transfer, or quenching of Br* by NO:



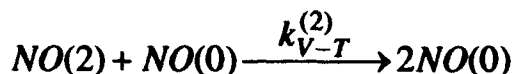
Quenching by molecular bromine:



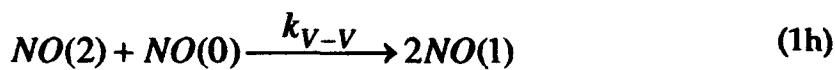
NO radiative decay:



V→T transfer, or NO self-quenching:



V→V transfer:



The rate for deactivation through collision with the chamber walls has been included in the radiative decay terms, Γ .

There are several other possible reactions that have been neglected due to very low reaction rates or populations of reactants. For example, it is entirely possible that collisions between Br^* and $NO(2)$ could produce $NO(3)$ or $NO(4)$. Based on Johnson's results, it is known that at most 10% of the bromine is in atomic form at any given time. Although Br^* and Br are produced in nearly equal proportions, the decay rate for Br^* is on the order of a thousand times faster than the recombination rate, so nearly all of the atomic bromine will be in

the ground state. Johnson found the total Br^* concentration to make up only about 0.4 percent of the total bromine pressure.⁽³⁾ The relative populations of any of the excited species must therefore be fairly low. It is therefore assumed that collisions between two excited species are infrequent, and do not contribute significantly to the overall distribution.

One other notable path that has been excluded from this mechanism is the possible quenching of $NO(2)$ to $NO(1)$, rather than to the ground state. This could occur through collision with either NO , Br_2 , or the wall. This was excluded based on previous studies, which indicate that the production of $NO(1)$ via quenching of $NO(2)$ will be most likely dominated by the fast V-V transfer rate, regardless of this incomplete quenching reaction.

These reaction equations can be used to write the rates for production and loss of the reactants.

$$\begin{aligned} \frac{d[Br^*]}{dt} = & k_{\text{pump}} I_{\text{pump}} [Br_2] - \Gamma_{Br} [Br^*] - k_Q^{(Br)} [Br_2] [Br^*] \\ & - (k_1 + k_2) [NO(0)] [Br^*] \end{aligned} \quad (2.a)$$

$$\begin{aligned} \frac{d[NO(1)]}{dt} = & k_1 [Br^*] [NO(0)] + 2k_{V-V} [NO(0)] [NO(2)] + \Gamma_2 [NO(2)] \\ & - \Gamma_1 [NO(1)] - k_Q^{(1)} [NO(1)] [Br^*] - k_{V-T}^{(1)} [NO(1)] [NO(0)] \end{aligned} \quad (2b)$$

$$\begin{aligned} \frac{d[NO(2)]}{dt} = & k_2 [Br^*] [NO(0)] - k_{V-V} [NO(0)] [NO(2)] - \Gamma_2 [NO(2)] \\ & - k_Q^{(2)} [NO(2)] [Br^*] - k_{V-T}^{(2)} [NO(2)] [NO(0)] \end{aligned} \quad (2c)$$

These can be simplified by two assumptions. First, if we assume that the number of particles that are excited is much less than the total number of particles, then we can make the approximation that the number in the ground state is a constant. Secondly, the fact that this experiment was conducted under steady-state conditions allows us to assume that all the rates of change are zero, so the equations can be solved algebraically to give the following:

$$[Br^*] = \frac{k_{\text{pump}} I_{\text{pump}} [Br_2]}{\Gamma_{Br} + k_Q^{(Br)} [Br_2] + (k_1 + k_2) [NO(0)]} \quad (3a)$$

$$[NO(1)] = \frac{k_1 [NO(0)] [Br^*] + 2k_{V-V} [NO(0)] [NO(2)] + \Gamma_2 [NO(2)]}{\Gamma_1 + k_Q^{(1)} [Br_2] + k_{V-T}^{(1)} [NO(0)]} \quad (3b)$$

$$[NO(2)] = \frac{k_2 [NO(0)] [Br^*]}{\Gamma_2 + k_Q^{(2)} [Br_2] + k_{V-T}^{(2)} [NO(0)] + k_{V-V} [NO(0)]} \quad (3c)$$

Note the coupling between $[NO(2)]$ and $[NO(1)]$ that appears in the numerator of the $[NO(1)]$ expression. This is a result of reactions that depopulate the $v = 2$ state by relaxing to the $v = 1$ state rather than the ground state. The radiative decay and $V \rightarrow V$ relaxation terms obviously behave this way, but it is possible that quenching of $v = 2$ by the molecular bromine could populate $v = 1$ as well. As mentioned before, it is believed that the $V \rightarrow V$ rate will completely dominate

this term, so it is assumed that the product of quenching by molecular bromine is the ground vibrational state.

D. Analysis Methods

1. Bromine Self-Quenching Rate.

The intensity observed from the side fluorescence will be proportional to the Einstein A coefficient for spontaneous emission times the population in the excited state, scaled by some constant factor, η , which includes such things as detector response and absolute radiometry factors. Recalling the expression for the Br^* population from the previous section, we can then write an expression for the intensity observed from Br^* in the absence of NO.

$$I_{\text{Br}^*} = \eta \frac{k_{\text{pump}} I_{\text{pump}} [\text{Br}_2]}{\Gamma_{\text{Br}} + k_Q^{(\text{Br})} [\text{Br}_2]} \quad (4)$$

If the fluorescence intensity is normalized by the pump intensity and the bromine concentration and then inverted, the result is

$$\frac{[\text{Br}_2]}{(I_{\text{Br}^*}/I_{\text{pump}})} = \frac{\Gamma_{\text{Br}}}{\eta k_{\text{pump}}} + \frac{k_Q^{(\text{Br})}}{\eta k_{\text{pump}}} [\text{Br}_2] \quad (5)$$

The quantity on the left side of this equation, bromine pressure over normalized bromine signal, will clearly show a linear dependence on bromine pressure. If this quantity is plotted against pressure, the ratio of the slope to the intercept of the line will give the quantity $k_Q^{(\text{Br})}/\Gamma_{\text{Br}}$. It is at this point necessary to know

either the bromine self-quenching rate, or Γ_{Br^*} which is the sum of the decay rate and the rate for deactivation by collision with the chamber wall.

The radiative decay of bromine is well established, but the collisions with the wall are obviously dependent upon the physical setup, so this number is not known. For this study, the value of $k_Q^{(Br)} = 1.2 \times 10^{-12} \text{ cm}^3/\text{molec-sec}^{(1,3)}$ will be used. This choice is based on both the agreement between Houston's and Johnson's measurements of this number and the fact that much of the apparatus used in this study was the same as that used by Johnson for his determination of this number.

2. Br^* Quenching by NO.

By examining the intensity of Br^* with NO in the reaction chamber, we can determine the total quenching rate of NO on Br^* . Since nearly all of the $E \rightarrow V$ transfer reactions populate either $v = 1$ or $v = 2$, this quenching rate is approximately equal to the sum $(k_1 + k_2)$. The intensity of Br^* in the presence of NO is given by

$$I_{Br^*} = \eta \frac{k_{\text{pump}} I_{\text{pump}} [Br_2]}{\Gamma_{Br} + k_Q^{(Br)} [Br_2] + (k_1 + k_2) [NO(0)]} \quad (6)$$

If reciprocal of the normalized intensity is plotted against NO pressure, the result is of course again linear

$$\frac{1}{(I_{Br^*}/I_{\text{pump}})} = \frac{\Gamma_{Br} + k_Q^{(Br)}[Br_2]}{\eta k_{\text{pump}}[Br_2]} + \frac{(k_1 + k_2)[NO(0)]}{\eta k_{\text{pump}}[Br_2]} \quad (7)$$

A similar analysis of slope to intercept ratio yields the quantity $(k_1 + k_2)$ in terms of quantities that have been determined previously.

3. Analysis of NO fluorescence.

Analysis of the observed fluorescence from the NO is much more complicated. It was earlier stated that the fluorescence from some excited state would be the population in that state times the radiative decay rate times some scaling factor involving detector response, and radiometry factors. For the NO intensity, there are contributions from two different excited states with different populations and decay rates. Furthermore, the detector that was used in this experiment had a different response at the two wavelengths of interest. This gives rise to the relation

$$I_{NO}^{(total)} = D_{5.3}A_{10}[NO(1)] + D_{5.4}A_{21}[NO(2)] \quad (8)$$

where the D coefficients contain both the detector response at the two wavelengths and the absolute radiometry factors, and $[NO(1)]$ and $[NO(2)]$ are given by equations 3b and 3c. When the cold NO filter is placed between the chamber and the detector, however, the absorption of the transition to the ground state will change the response of the detector system at 5.3 microns, but

not cause much change at all at 5.4 microns. This provides us with a second equation.

$$I_{NO}^{(cf)} = D_{5.3}^{(cf)} A_{10} [NO(1)] + D_{5.4}^{(cf)} A_{21} [NO(2)] \quad (9)$$

At this point, if the D coefficients are determined, then the problem of finding the populations in the two vibrational levels is reduced to a simple matter of solving a system of two equations with two unknowns. In practice, these D coefficients contain absolute radiometry factors which make them difficult to determine absolutely, so they are determined relative to one another.

By defining some constants to express these coefficients relative to $D_{5.3}$,

$$a_{5.4} \equiv \frac{D_{5.4}}{D_{5.3}} \quad (10a)$$

$$a_{5.3}^{(cf)} \equiv \frac{D_{5.3}^{(cf)}}{D_{5.3}} \quad (10b)$$

$$a_{5.4}^{(cf)} \equiv \frac{D_{5.4}^{(cf)}}{D_{5.3}} \quad (10c)$$

the ratio of the observed fluorescence intensity with the cold NO filter to the intensity without the filter can be written in terms of measurable quantities

$$\frac{I_{NO}^{(c.f.)}}{I_{NO}^{(total)}} = \frac{(A_{10}/A_{21})a_{5.3}^{(c.f.)}[NO(1)] + a_{5.4}^{(c.f.)}[NO(2)]}{(A_{10}/A_{21})[NO(1)] + a_{5.4}[NO(2)]} \quad (11)$$

If the expressions for the excited NO populations from equation 3 are used, and the terms are grouped according to their dependence upon the NO concentration, this ratio of intensities takes on the following functional form

$$\frac{I_{NO}^{(c.f.)}}{I_{NO}^{(total)}} = \frac{A[NO(0)] + 1}{B[NO(0)] + C} \quad (12)$$

The A and B coefficients contain enough terms to make it very difficult to extract much information from them. The C coefficient, on the other hand, is a bit more tractable:

$$C = \frac{(A_{21}/A_{10})a_{5.4}^{(c.f.)}}{(A_{21}/A_{10})a_{5.4} + \frac{k_1}{k_2}(L_2/L_1)} \quad (13)$$

Where L_n , the total loss term for species n, is the sum of the terms which represent destruction of species n (radiative decay and collisional quenching reactions). Notice that if the ratio in equation 12 is plotted against NO pressure, the intercept (limit as [NO] approaches zero) is $1/C$. By fitting this form to the data, the constant C can be determined. With a few assumptions about the loss terms, this gives us the branching ratio k_1/k_2 .

III EXPERIMENT

A. Experimental Setup

1. Main Apparatus.

The main apparatus used in this experiment is shown below in figure 1. A Spectra Physics model 165 argon-ion laser operating at 488.0 nm and producing from 1.0 to 1.5 Watts of continuous power was used to photodissociate molecular

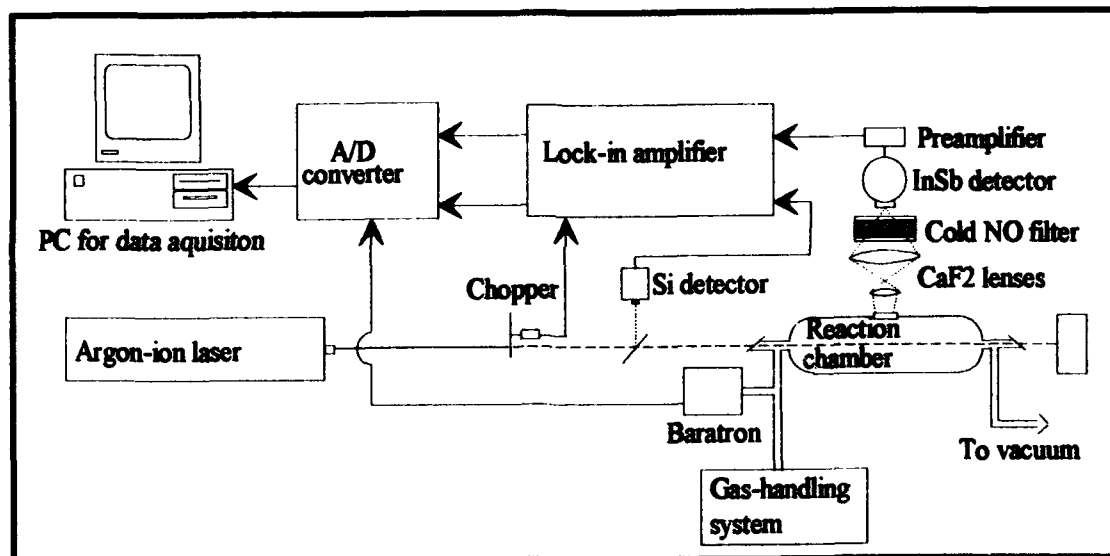


Fig 1: Experimental apparatus.

bromine. The laser was passed through a Stanford Research SR540 chopper running at 200 to 225 Hz and then into the reaction chamber.

The chamber was composed of a glass cylinder 16 inches long by 2 inches outside diameter. The cylinder narrowed to 1/2 inch diameter at the ends, where

Pyrex Brewster windows were connected via Cajon Ultra-Torr fittings. The gas inputs, exhaust to vacuum, and an MKS 10 Torr Baratron were also connected into the chamber at these joints. The NO fluorescence was observed through a 1 inch diameter CaF_2 window in the side of the chamber. The radiation was focused onto the detector element by two CaF_2 (focal lengths 2 and 4 inches) lenses, and passed through an OCLI bandpass filter which transmitted radiation from both of the NO vibrational transitions. The spectral response of the filter over the usable range of the detector is shown in figure 2. The response

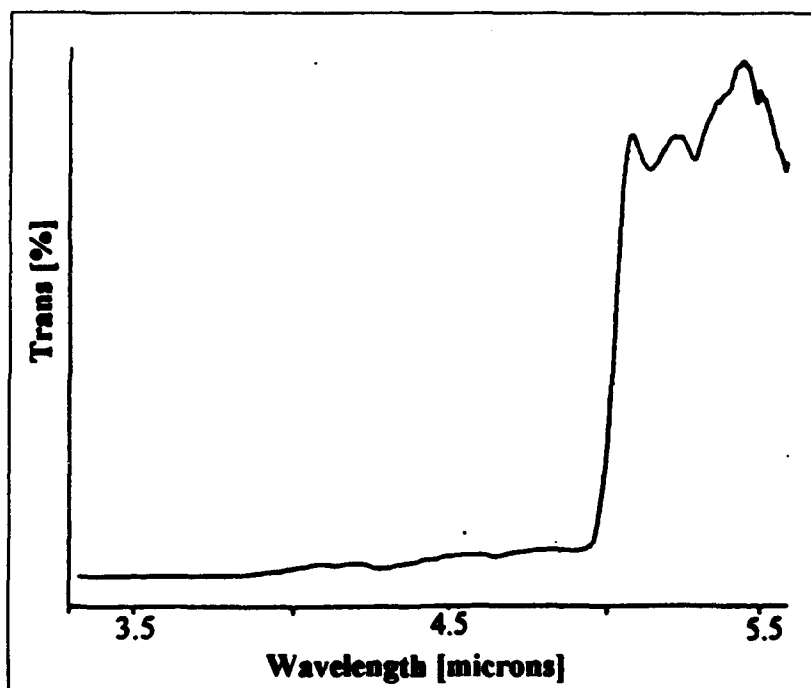


Fig 2: Measured transmittance of 5.0 micron long-pass filter used for observations of NO fluorescence.

of the detector itself also limited the wavelengths that were observed. This is shown in figure 3. In addition, a cell containing about 1 Atm of room

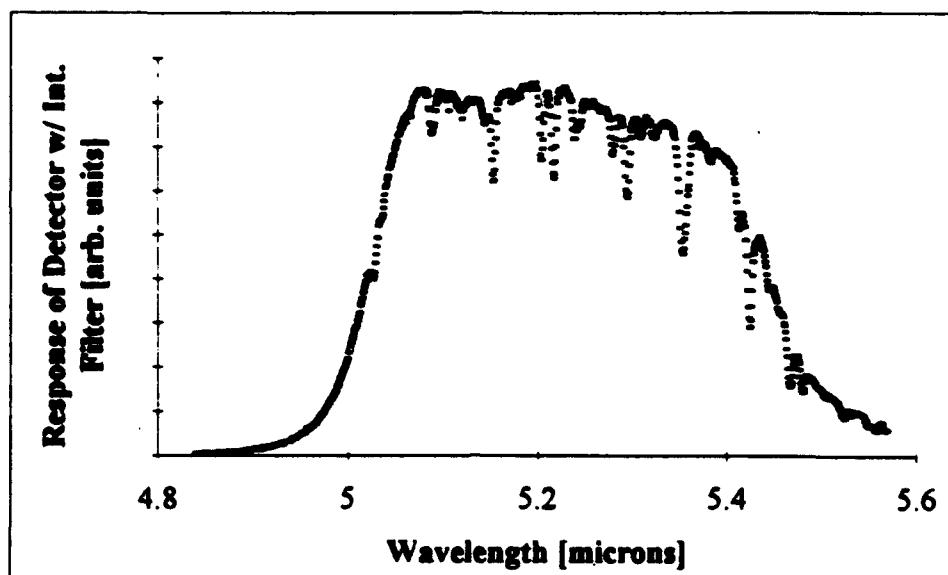


Fig 3: Response curve for the InSb detector, as measured.

temperature NO could be placed between the lenses and the detector to selectively absorb the $v = 1 \rightarrow v = 0$ transition. This cold filter had an absorption length of 1 inch, with 2 inch diameter CaF_2 windows.

The spectral response of the detector was determined using a Jarrell-Ash grating monochromator, along with an Electro-Optics Industries black-body calibration source. The setup used for this experiment is shown below in figure 4. The effect of the interference filter and the cold NO filter was measured in a Bomem DA8 FTIR spectrophotometer. The transmission of the cold NO filter is provided in appendix B.

The detector was an EG&G Judson InSb photovoltaic detector with a 2mm diameter active area. The output of the detector was sent to an EG&G PA-9 matched preamplifier (AC coupled) and then to a Stanford Research model 510

lock-in amplifier. The voltage input to the preamplifier came from a Hewlett Packard model 6236B Triple Output power supply.

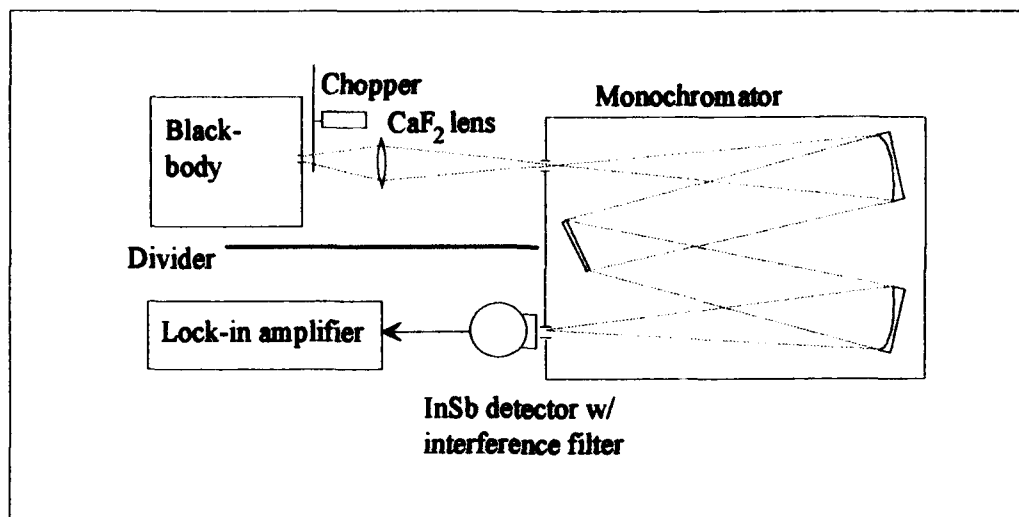


Fig 4: Apparatus used for measurement of detector response.

Relative laser power was continuously monitored using an FND-100 photodiode and an SR510 lock-in amplifier. The absolute power was measured with Coherent model 210 power meter in the main beam.

Outputs from the pressure transducer and from the lock-in amplifiers were sent to a Quinn-Curtis DAS-8 A/D converter card via BNC coaxial cable, and then into a 386SX PC. Data acquisition was managed by Turbo Lablog, a program by Metrabyte.

The bromine was supplied by Spectrum Chemical Manufacturing Corporation, and was 99.5% pure. The nitric oxide was from Matheson, with a purity of 99.0%.

2. Gas Handling System.

A schematic of the gas handling system is shown below in figure 5. The system was composed of several types of tubing. A combination of 1/2 inch stainless steel flex-tube and Kontes 1/2 inch outside diameter glass-teflon valves was used for the bromine supply and for the exhaust to the vacuum pump. This tubing was connected using 1/2 inch Cajon Ultra-Torr fittings. The nitric oxide supply used 1/4 inch Teflon tubing, connected by Swagelok fittings. These came together in the mixing manifold, which was 1/4 inch stainless steel tubing

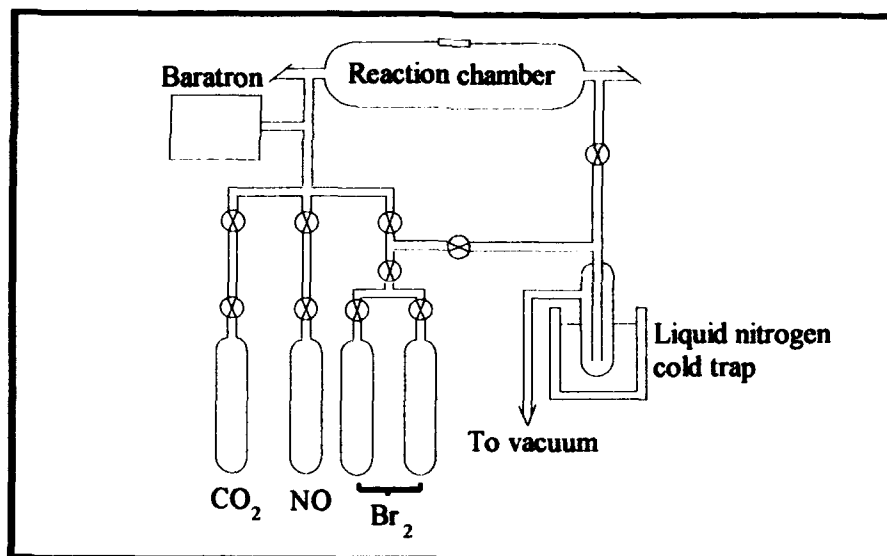


Fig 5: Gas handling system.

connected by with Swagelok fittings. Flow was controlled in the mixing manifold by a combination of Nupro ball valves and needle valves. All supply lines had at least two valves between the source and the reaction chamber for an

"airlock" effect. All glassware other than Kontes tubing was custom manufactured by Mike Ray, of the Wright Laboratories glass shop.

B. Experimental Procedures

1. Bromine Distillation.

Of all the contaminants readily available in the atmosphere, only CO_2 and water have any sort of cross-section for absorbing the IR signal, or for quenching the Br^* and reemitting in the IR. These two contaminants are fairly simple to remove in a freeze-thaw distillation. Other contaminants could quench Br^* , but since the absolute pump rate is not important to this study, small amounts of quenching are tolerated.

When distilling, the bromine was first placed into one of two bulbs which could either be connected to vacuum or to each other. The bulb containing the bromine was placed in liquid nitrogen to freeze the bromine, and then the system was opened to the vacuum. The bromine was then allowed to thaw. Carbon dioxide has a boiling point much lower than that of bromine, so as the frozen mixture warmed, the CO_2 evaporated first. The system was kept under vacuum during this first phase to remove the CO_2 as it boiled off. The pressure was monitored to estimate when the CO_2 had been exhausted, and the system was then sealed off from the vacuum. At this point, the empty bulb was placed in liquid nitrogen to condense the bromine vapor as it boiled. Bromine has both

a lower boiling point than water, and a higher vapor pressure, so as long as there was still liquid bromine in the first bulb, all of the water was still liquid. The last bit of bromine was discarded to ensure that none of the water remained.

2. Detector Alignment.

Detector alignment was generally done in two stages, first using a visible signal for gross alignment, and then a mixture of Br_2 and CO_2 for fine adjustments.

First, the reaction chamber was opened to atmosphere and filled with an aerosol to scatter the blue-green light from the laser. The scattered light could then be seen imaged onto the face of the detector. Because the index of refraction is different at 488nm than in the mid-IR, this method could only be used to get the alignment close.

If this was done carefully, the alignment would be close enough that some signal would fall onto the detector, which could then be used for more precise adjustment, as well as setting the phase of the lock-in amplifier. For this fine tuning, a mixture of Br_2 and CO_2 was used, because it gives a very strong signal at 4.3 microns. This was done using a different filter, which had a narrow bandpass at 2.7 microns as well as a long pass window from about 4.0 microns to well past the cutoff of the detector response. This passed radiation from both Br^* and CO_2 .

C. Experiments Performed

1. Br^* Lifetime.

The goal of the first experiment was to determine rate for deactivation of Br^* due to radiative decay and collisions with the wall. According to equation 5, the analysis calls for a graph of inverse bromine fluorescence intensity vs bromine pressure. To achieve this, the reaction chamber was first evacuated and allowed to outgas until a minimum pressure had been attained (< 10 mTorr). The laser was then turned on and allowed to warm up for several minutes, until output power stabilized. Bromine was then slowly leaked into the chamber through a needle valve at a rate of a few mTorr/sec. The fluorescence intensity, relative laser intensity, and total pressure were all recorded once per second by the computer. A typical data run covered a range of less than 5 Torr, and lasted from 15 to 25 minutes.

2. $E \rightarrow V$ Transfer Rate.

The goal of the next part of the experiment was to determine the total quenching rate for NO on Br^* . For this, a graph of inverse bromine intensity versus NO pressure was needed, for some known pressure of bromine (cf. equation 7). After the chamber was evacuated, some amount of Br_2 (generally between 0.5 and 4.0 Torr) was placed in the chamber. After the bromine source

was closed off, the total pressure in the chamber was observed to steadily drop, until some equilibrium pressure had been achieved. Pressure drops were generally a couple hundred mTorr. This is attributed to bromine absorbing onto the chamber walls.⁽³⁾ In this experiment the bromine pressure was allowed to settle out to equilibrium before the data run was begun. At this time, the NO was slowly leaked into the chamber, and the bromine intensity was observed as before.

3. Branching Fraction for $E \rightarrow V$ Transfer.

The main goal of the experiment was to determine the branching ratio for NO on Br*. This was done in three steps. First, the total NO fluorescence (including both the 5.33 and the 5.41 micron radiation) was observed versus NO pressure in the same manner as described above. Next, a monochromator scan of a block-body calibration source was used to find the relative response of detector-interference filter combination at the wavelengths of interest. This allowed for a more precise determination than was possible by interpolating the manufacturer's detector response curve. Lastly, the effect of the cold NO filter was estimated using the FTIR spectrometer.

The measurements of the fluorescence were performed in a similar manner to that described above. The NO was slowly leaked into a chamber containing some fixed amount of Br₂. This was repeated for several different

bromine pressures, ranging from 0.5 Torr to 4.0 Torr. An upper limit was placed on the Br_2 pressure by the A/D converter card, which was only capable of accepting inputs up to 5.0 Torr. For each concentration of Br_2 , the experiment was conducted both with and without the cold NO filter in place.

As has been discussed before, the room temperature NO should absorb the radiation from the $1 \rightarrow 0$ transition (around 5.33 microns) very strongly, while transmitting most of the 5.41 micron radiation from the $2 \rightarrow 1$ transition. This simple model is complicated by the fact that there is some rotational distribution associated with these transitions, so the two transitions have some overlap. Because the thermal population in $v > 0$ states in NO is very nearly zero at room temperature, the only absorption of the $2 \rightarrow 1$ transition comes from overlap of the rotational spectra for the two transitions. Where the P branch of the $2 \rightarrow 1$ transition overlaps with the R branch of the $1 \rightarrow 0$ transition, the $v=2 \rightarrow v=1$ radiation can actually be absorbed by molecules in the ground state.

The rotational spectrum of the $v=1 \rightarrow v=0$ transition is shown in appendix B. These are from FTIR measurements of the transmission of the cold NO filter. Notice that the transmission is zero at all of the allowed transition wavelengths. This means that the $1 \rightarrow 0$ transition is completely absorbed by the cold NO filter, which tells us that $D_{5,3}^{(c.f.)} = 0$.

The overlap of the two rotational spectra was estimated by using published values for the coefficients to the Dunham expansion^(14,15) to produce a

stick spectrum for the 2→1 transition, and assuming a thermal rotational distribution. The transitions that overlapped a spike in the 1→0 spectrum were weighted by their thermal population and by the detector response at that wavelength, and then summed to estimate what fraction of the 2→1 transition would be absorbed by ground vibrational state molecules, which is the equal to the ratio of $D_{5.4}^{(c.f.)}$ to $D_{5.4}$.

The detector response that was used for this calculation and for comparing $D_{5.4}$ to $D_{5.3}$ came from observations of a black-body source resolved by a grating monochromator as described previously. A piecewise-linear interpolating function was used for this comparison.

During observations of the fluorescence with the cold NO filter, a combination of the low detector response at 5.41 microns and the absorption of the 5.33 micron signal by the cold filter made the fluorescence observed through the cold filter very low. In order to maintain the output of the lock-in amplifier in a range that was allowed by the A/D converter card, a higher sensitivity was used when observing the fluorescence through the cold filter. The amplifier was ten times more sensitive in this phase than in the unfiltered observations, so the data without the cold filter has been multiplied by ten to correct for the different scale.

In order to verify that this produced the same scale as the higher sensitivity, a data run was performed using two amplifiers: one with a low

sensitivity and one with a sensitivity ten times higher than the first. The output of the low sensitivity amp was multiplied by ten and graphed along with the output of the high sensitivity amp. The result, shown below in figure 5, demonstrates that the output does in fact scale as the sensitivity of the amplifier.

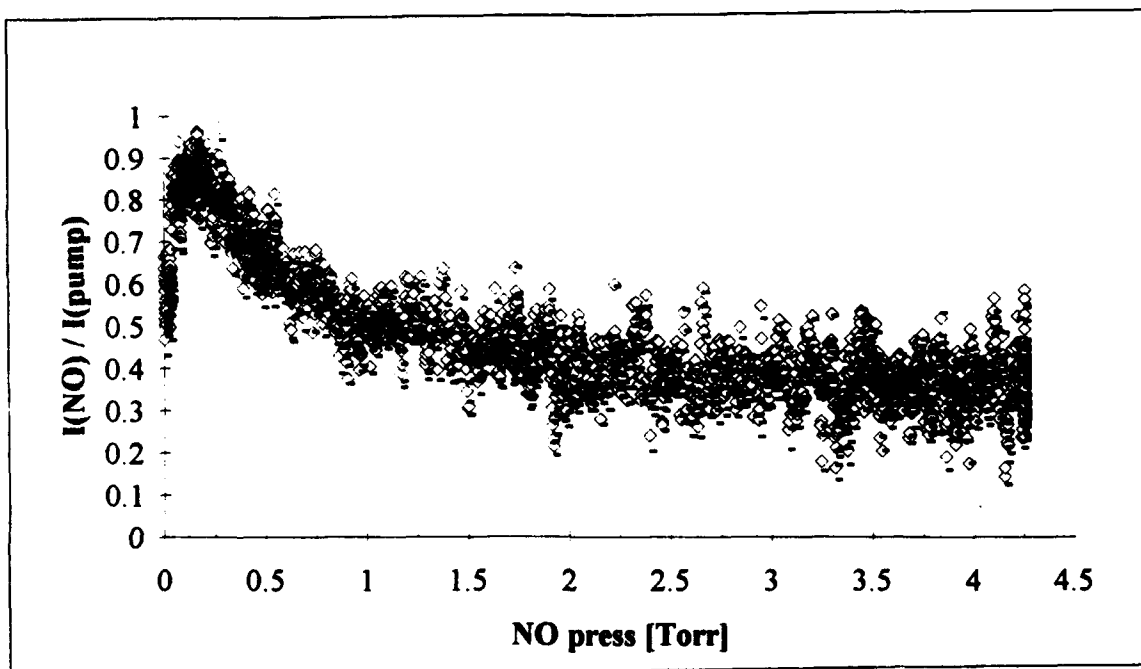


Fig 6: Comparison of amplifier response. Diamonds show high sensitivity amplifier output; dashes show low sensitivity amplifier output multiplied by the ratio of sensitivities.

IV. RESULTS

A. Introduction

This section outlines the results of this research. Data are presented, and the analysis techniques discussed earlier are applied. Recommendations for future research are also provided.

B. Quenching Rates for Br_2 and NO on Br^*

The observed Br^* fluorescence intensity, normalized by the relative pump intensity, is shown as a function of Br_2 pressure below in Figure 7. The plot showed an unexpected decrease in fluorescence with increasing bromine pressure. Since the mechanism contains no factors that could account for this behavior, this was explained by absorption of the pump beam.^(3,13) The active viewing volume of the detector falls at the midpoint of the reaction chamber, so the pump beam was attenuated by absorption through 8 inches of bromine before reaching an area that could be seen with the detector. Beers law for absorption says that the intensity observed after traveling a distance z through a medium with some cross section for absorption σ is given by

$$I(z) = I(0) \exp[-\sigma zN]$$

where N is the concentration of the absorbing particles. To correct for the absorption of the pump beam, the intensity is normalized by $I(z)$, rather than

$I(0)$. The cross section used for this calculation was $4.13 \times 10^{-19} \text{ cm}^2$.⁽³⁾ This corrected data is also shown in figure 7, along with the uncorrected data.

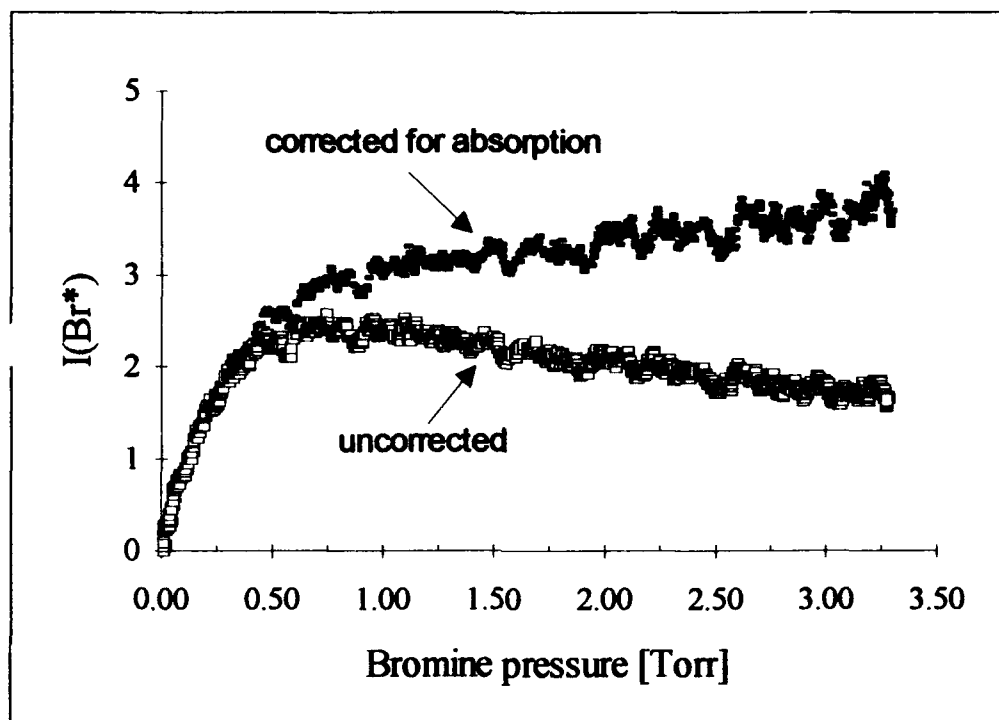


Fig. 7: Bromine fluorescence as a function of bromine pressure with no NO present, corrected for absorption of the pump laser

The Stern-Volmer plot for this data is shown below in figure 8. As discussed earlier in chapter 2, the ratio of the slope to intercept of this plot is equal to the ratio of $k_Q^{(Br)} / \Gamma_{Br}$. This ratio was found to be 3.48 ± 0.13 . Using Johnson's value for bromine self-quenching of $1.2 \times 10^{-12} \text{ cm}^3/\text{molec-sec}$,⁽³⁾ this yields a value of $\Gamma_{Br} = (1.25 \pm 0.15) \times 10^4 \text{ sec}^{-1}$, which compares well with Johnson's value of 1.19×10^4 . As this term includes factors that are dependent on the physical setup

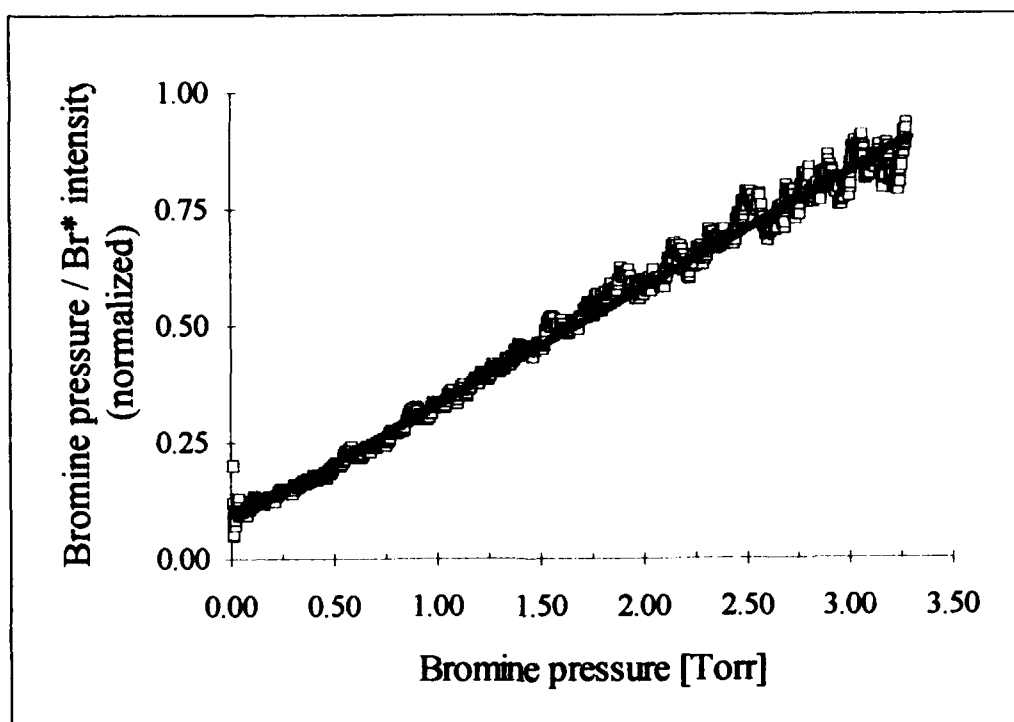


Fig 8: Stern-Volmer plot for Br* fluorescence, in the absence of NO

of the chamber and most but not all of the apparatus used was from Johnson's experiment, it is reasonable to expect these numbers to be close, but not necessarily equal.

A second observation of Br* fluorescence intensity was made, this time with a fixed concentration of bromine and a varying amount of nitric oxide. It was not necessary to correct for the pump beam absorption in this case, since there was no change in bromine pressure and the absolute pump rate is not important for this analysis. The inverse Br* fluorescence is shown below as a function of NO pressure, in the presence of 2.0 Torr of Br₂.

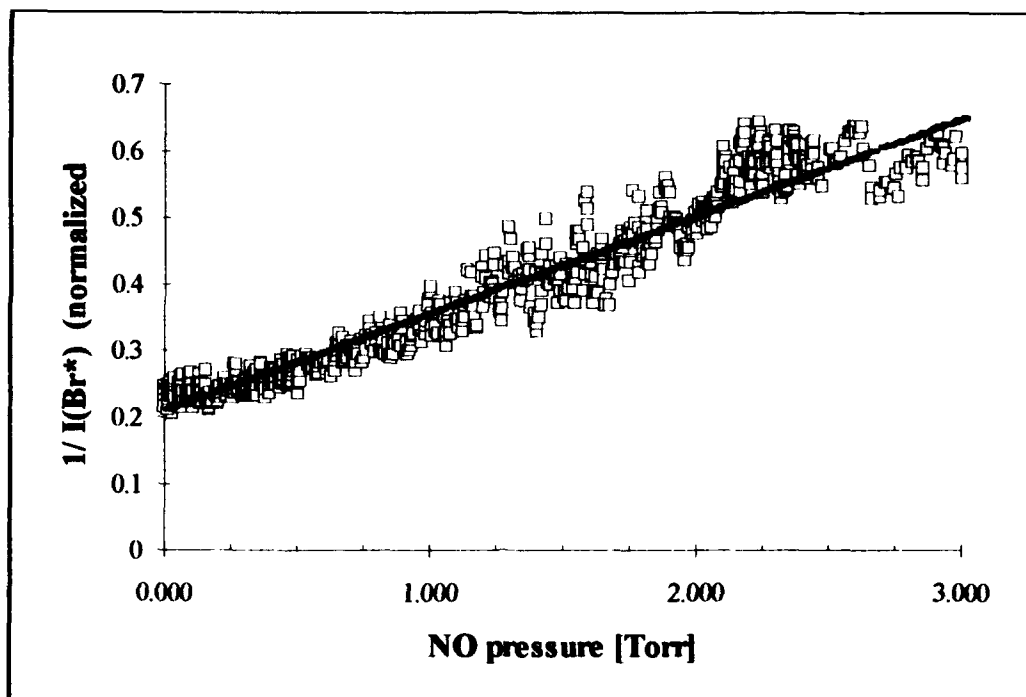


Fig 9: Inverse Br* signal vs. NO pressure, in the presence of 2.0 Torr Br₂

The slope to intercept ratio for this data is 0.688 ± 0.017 . From equation 7, the slope to intercept ratio is equal to the ratio $(k_1 + k_2)/(\Gamma_{Br} + k_Q^{(Br)}[Br_2])$. The value of $(\Gamma_{Br} + k_Q^{(Br)}[Br_2])$ at 2.0 Torr of Br₂ is $8.88 \times 10^4 \text{ sec}^{-1}$, which gives a value of the total quenching rate of NO on Br* of $(1.9 \pm 0.2) \times 10^{-12} \text{ cm}^3/\text{molec-sec}$.

C. NO Fluorescence Data

A typical profile of NO fluorescence as a function of NO pressure is shown below in figure 10, both with and without the cold NO filter in place. In this graph, the intensity observed with the filter has been multiplied by 10 to

show detail. For similar graphs at different bromine pressures, the reader is referred to Appendix C. The observed intensity with the filter in place is

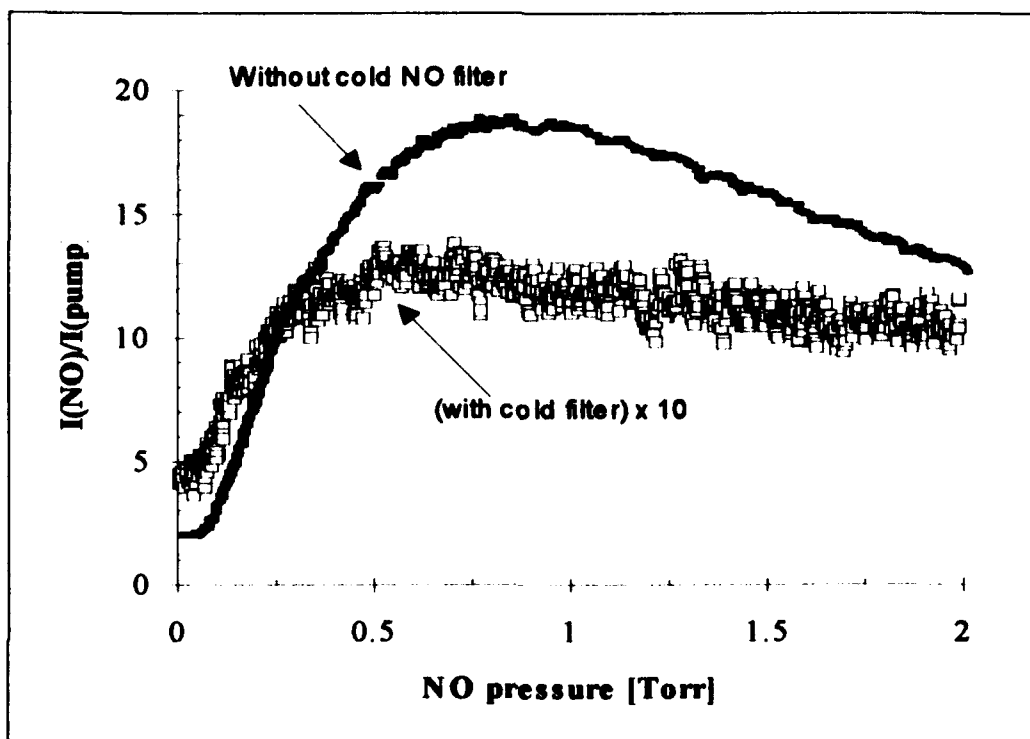


Fig 10: NO fluorescence vs NO pressure with 3.0 Torr bromine, with and without cold NO filter in place

roughly an order of magnitude less than without the filter. This implies that nearly all of the signal observed without the filter is from the $1 \rightarrow 0$ transition. NO lasers operating on the $2 \rightarrow 1$ transition have been demonstrated,^(3,6) so there must be more population in $v = 2$ than in $v = 1$. The most likely explanation for this data is that the detector response at 5.41 microns is much smaller than that at 5.33 microns.

The observed NO fluorescence without the cold filter in place for several different bromine pressures is shown below in figure 11 . Because the detector response at 5.3 microns is so much higher than at 5.4, this fluorescence is almost entirely from the 1→0 transition.

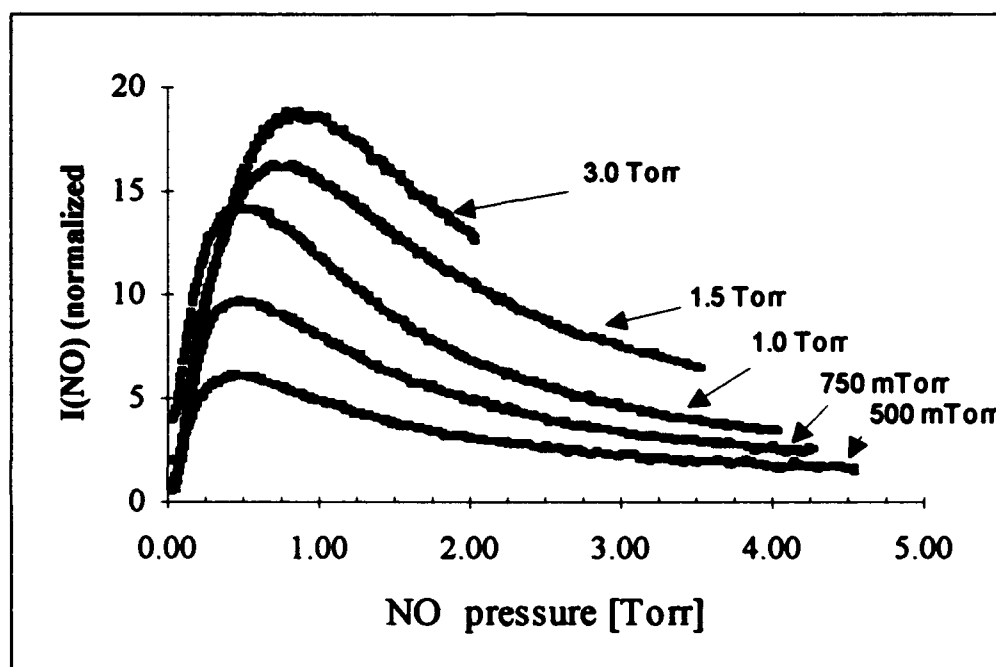


Fig 11: NO fluorescence vs. NO pressure for several different bromine pressures

As discussed previously, taking the ratio of the cold filtered fluorescence data to the unfiltered data should allow us to find the branching fraction. In order to take this ratio of intensities, it was necessary to assume a functional form for one of the sets of data points to find an interpolating function, and then ratio the value of the other set of data against this interpolating function. The functional form

$$I_{NO}^{(c.f.)} = \frac{\alpha [NO(0)]}{(\beta [NO(0)] + 1)(\gamma [NO(0)] + 1)}$$

was used to interpolate the data for the fluorescence observed through the cold NO filter. For details of the derivation of this form, see Appendix D. The coefficients of this form were chosen by TableCurve (Jandel Scientific Inc.) to minimize the mean squared error. By taking the ratio of the unfiltered data to this function, the following plot of $I^{(c.f.)}/I^{(total)}$ (for 3.0 Torr of Br_2) was produced.

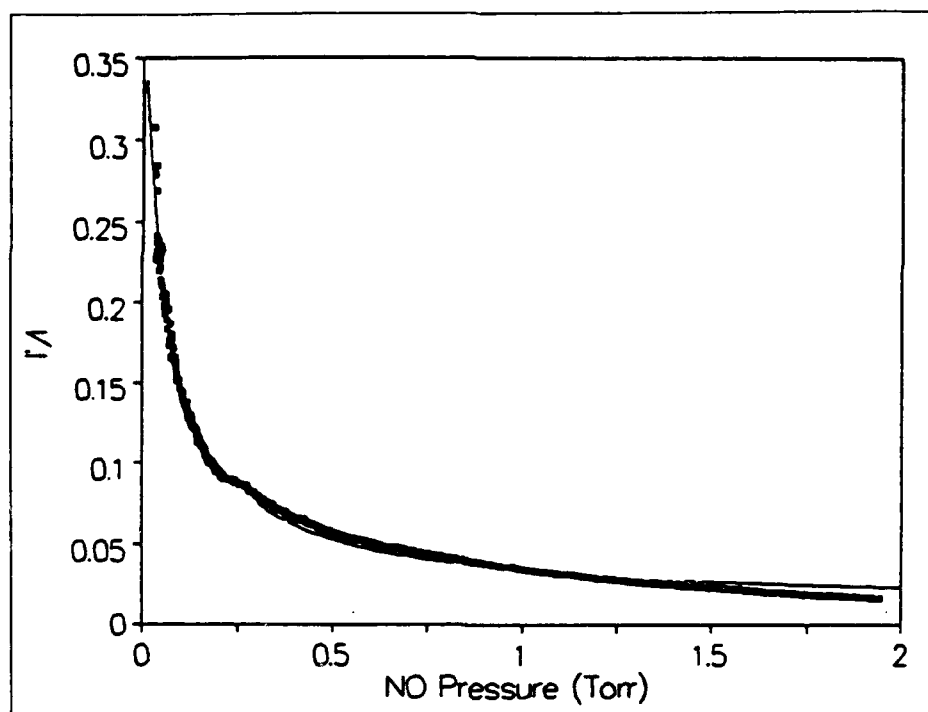


Fig 12: Ratio of observed intensity with the cold NO filter to observed intensity without the filter, for 3.0 Torr of Br_2 .

By averaging the zero-pressure intercept of this line, $1/C$, over bromine pressure, the average value of C was found to be 2.4 ± 0.4 (averaged over bromine pressure). From chapter two, we had

$$C = \frac{(A_{21}/A_{10})a_{5.4}^{(cf)}}{(A_{21}/A_{10})a_{5.4} + \frac{k_1}{k_2}(L_2/L_1)}$$

A_{21}/A_{10} is known to be about 1.9. From the piecewise linear approximation to the detector response curve, $a_{5.4} = 0.73 \pm 0.02$. Lastly, from the estimate of the overlap of the two rotational distributions, we find $a_{5.4}^{(c.f.)} = 0.33 \pm 0.04$.

It is now necessary to make a few assumptions about the loss terms, L_n . One reasonable assumption would be that the decay rates out of the two vibrational states follow Landau-Teller scaling, which predicts that the rate out of $v = 2$ will be roughly twice the rate out of $v = 1$ (i.e., $L_2/L_1 \approx 2$). It is also possible that there is no scaling rule for NO, so the rates should be approximately equal for the two states ($L_2/L_1 \approx 1$). At this time, it is not known which of these two assumptions is correct.

Depending on the initial assumptions about these depletion terms, the branching ratio, k_1/k_2 , is found to be only about 10%. This agrees well with the result of the laser demonstration. The branching fraction, $k_2/(k_1+k_2)$, is more useful for comparison to other published values, and also makes the possibility for achieving inversion more clear. The branching fraction, for the case of no

scaling, is found to be 0.89 ± 0.21 . By assuming the extreme cases (limit of the uncertainty of each measurement) of all values in this expression, it is found that the branching fraction can be no less than 0.68, and can obviously be no greater than one. If, on the other hand, Landau-Teller scaling is assumed, the branching ratio is found to be 0.94, which is well within the uncertainty of the no-scaling case.

D. Conclusions

1. *Recommendations for Future Research.*

To explore the two lines of NO fluorescence properly, an HgCdTe detector should be used to eliminate the problem of the detector cutoff. This was attempted in this study, but the active area of the detector that was used was too small (0.04 mm^2) to obtain a useful signal level.

Wight used an HgCdTe detector with a 25 mm^2 active area in his study. His data is still surprisingly noisy, however. This could be a result of doing the experiment in a pulsed regime. The steady-state photolysis technique used in this report has been shown to produce very high quality data. If this could be reproduced on an HgCdTe detector, it would be possible to obtain a much more precise measurement of the branching fraction than Wight presented.

It would also be very helpful to know whether Landau-Teller scaling applies to this system or not. Although the answer to this question does not

affect the outcome greatly in this case, the lower uncertainty in measurements on the HgCdTe detector would make this choice important.

2. *Conclusions.*

The branching fraction, $k_2/(k_1+k_2)$, for E-V transfer from Br^* to NO was found to be 0.89 ± 0.21 . This agrees very closely with the previous value of 0.86 reported by Wight.⁽¹²⁾ The high quality of data in this experiment as well as the more comprehensive reaction mechanism give this result slightly more confidence than Wight's, even though the result is not significantly different.

V. BIBLIOGRAPHY

1. P. L. Houston. "Electronic to Vibrational Energy Transfer from Excited Halogen Atoms," *Advances in Chemical Physics*, Vol 47, edited by J. Jortner, R. D. Levine, and S. A. Rice. New York: Wiley and Sons, 1981.
2. A. B. Hariri and C. Wittig. "Electronic to Vibrational Energy Transfer from $\text{Br}(4^2\text{P}_{1/2})$ to CO_2 , COS , CS_2 ," *Journal of Chemical Physics*, 67: 4454-4462 (November 1977)
3. R. O. Johnson. "Excited Atomic Bromine Energy Transfer and Quenching Mechanisms," *Doctoral Dissertation, Air Force Institute of Technology (AU)*, August 1993
4. A. B. Peterson, A. B. Hariri, and C. Wittig. "Electronic-Vibrational Energy Transfer from $\text{Br}(4^2\text{P}_{1/2})$ to HCN and Deactivation of $\text{HCN}(001)^*$," *Journal of Chemical Physics*, 65: 1872-1875 (September 1976).
5. C. A. Taatjes, C. M. Lovejoy, B. J. Opansky, and S. R. Leone. "Laser Doubled Resonance Measurements of the Quenching Rates of $\text{Br}(4^2\text{P}_{1/2})$ with H_2O , D_2O , HDO , and O_2 ," *Report to Phillips Laboratory, Advanced Concepts Branch, Kirtland AFB, NM*, April 1991
6. A. B. Peterson, L. W. Braverman, and C. Wittig. " H_2O , NO , and N_2O Infrared Lasers Pumped Directly and Indirectly by Electronic-to-Vibrational Energy Transfer," *Journal of Applied Physics*, 48: 230-233 (January 1977)
7. R. J. Donovan and D. Husain. "Chemistry of Electronically Excited Atoms," *Chemical Reviews*, 70: 509-516 (1970).
8. R. F. Tate. "Steady-State Production and Quenching of $\text{Br}(4^2\text{P}_{1/2})$," *Masters Thesis, Air Force Institute of Technology (AU)*, October 1991.

9. S. R. Leone and F. J. Wodarczyk. "Laser-Excited Electronic-to-Vibrational Energy Transfer from $\text{Br}(4^2\text{P}_{1/2})$ to HCl and HBr," *Journal of Chemical Physics*, 60: 314 (January 1974).
10. H. Hoffman and S. R. Leone. "Collisional Deactivation of Laser-Excited $\text{Br}^*(^2\text{P}_{1/2})$ Atoms with Halogen and Interhalogen Molecules," *Chemical Physics Letters*, 54: 314-319 (March 1978).
11. V. S. Kushawaha. "Electronic-Vibrational Energy Transfer from Br^* to N_2O ," *Physica Scripta*, 20: 75-80 (1979)
12. C. A. Wight. "Infrared Fluorescence Studies of Near Resonant Electronic-Vibrational Energy Transfer Collisions: $\text{Br}(4^2\text{P}_{1/2}) + \text{NO}$," *Journal of Physical Chemistry*, 90: 2683-2687 (1986).
13. G. P. Perram. Professor, Air Force Institute of Technology (AU), personal interviews (April-September 1993).
14. N. L. Nichols, C. D. Hause, and R. H. Noble. "Near Infrared Spectrum of Nitric Oxide," *Journal of Chemical Physics*, 23: 57 (1955).
15. M. D. Olman, M. D. McNelis, and C. D. Hause. "Molecular Constants of Nitric Oxide from the Near Infrared Spectrum," *Journal of Molecular Spectroscopy*, 14: 62-78 (1964).
16. H. Okabe. *Photochemistry of Small Molecules*. New York: John Wiley and Sons, 1978

APPENDIX A: SPECTROSCOPIC NOTATION

A. Introduction

This appendix will review the spectroscopy of bromine. The notation used will be briefly explained, and the photolysis of molecular bromine will be discussed.

B. Atomic Bromine

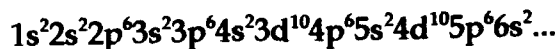
The energy of an atom can be described as the sum of the energy of translation of the nucleus plus the energy associated with the motion of the electrons. The set of quantum number n , l , m , and s describe the state of an electron and the energy associated with it. When an atom has more than one electron, however, the quantum numbers of all the electrons are summed to arrive at a symbol that describe the state of the entire electron cloud, rather than the individual electrons. This is referred to as the term symbol, and has the format

$$^{2S+1}L_J$$

where $\vec{S} = \sum \vec{s}$, $\vec{L} = \sum \vec{\ell}$, and $\vec{J} = \vec{L} + \vec{S}$. Because the angular momentum vectors have several possible orientations (several values of m_l), there are in general several configurations (and therefore several different energies) that are accessible to a given set of electrons. The ordering of the energies is given by

Hund's rules. The most important factor in determining the energy ordering is the quantity $2S + 1$, or the multiplicity. The higher the multiplicity, the lower the energy. For states with the same multiplicity, the angular momentum L determines the order. Again, higher values of L mean lower values of energy. Lastly, all other terms being equal, the value of J is the last factor. If the outermost energy level is less than half full, then higher J means higher energy. If this level is more than half full, then higher J means lower energy.

Bromine has 35 electrons. These fill subshells in the order given by the Aufbau principle, shown below.



where the superscript shows the number of electrons required to fill any given subshell. The thirty five electrons of bromine completely fill all of the subshells up through $3d^{10}$, and partially fill the $4p$ subshell with 5 electrons. Because the Pauli exclusion principle requires that a full subshell have as many electrons with negative values of m_l and m_s (the orientations of the orbital angular momentum vector and electronic spin, respectively) as with positive, any filled subshell will always sum to a total angular momentum of $J = 0$. All of these electrons can therefore be ignored, except for those in the $4p^5$ subshell.

For the same reason that a full subshell sums to zero, a subshell that can only accept one more electron is equivalent to a subshell with only one electron. For purposes of finding the term symbol then, ground state bromine has but one

p electron. This gives us a ground state term symbol of $^2P_{1/2}$ or $^2P_{3/2}$. According to Hund's rules, the $^2P_{3/2}$ will have the lowest energy. The $^2P_{1/2}$ has been found to be about 3685 cm^{-1} above that. If one of the other electrons in bromine were excited, we would no longer have a single p electron, and more states would be accessible to the atom.

3. Molecular Bromine and Photolysis

When two or more atoms come together to form a molecule, the result is an entirely new state, which describes the electron cloud surrounding the entire molecule. In addition to the energy of the electrons around a molecule, there can also be energy associated with vibration of nuclei and rotation. In general, any given electronic energy level will have dozens of vibrational levels associated with it, and each of these will have up to a hundred rotational levels. Typical vibrational splittings are on the order of hundreds of wavenumbers, while typical rotational splittings are a few wavenumbers.

Ground state bromine atoms are in a $^2P_{3/2}$ configuration, so we would expect the ground state for a bromine molecule to correspond two $^2P_{3/2}$ bromine atoms in the separated atom limit. For photolysis of bromine, we need a configuration in which at least one of the atoms is excited. Figure 11 below shows an energy diagram for molecular bromine. These curves represent only the electronic energy.

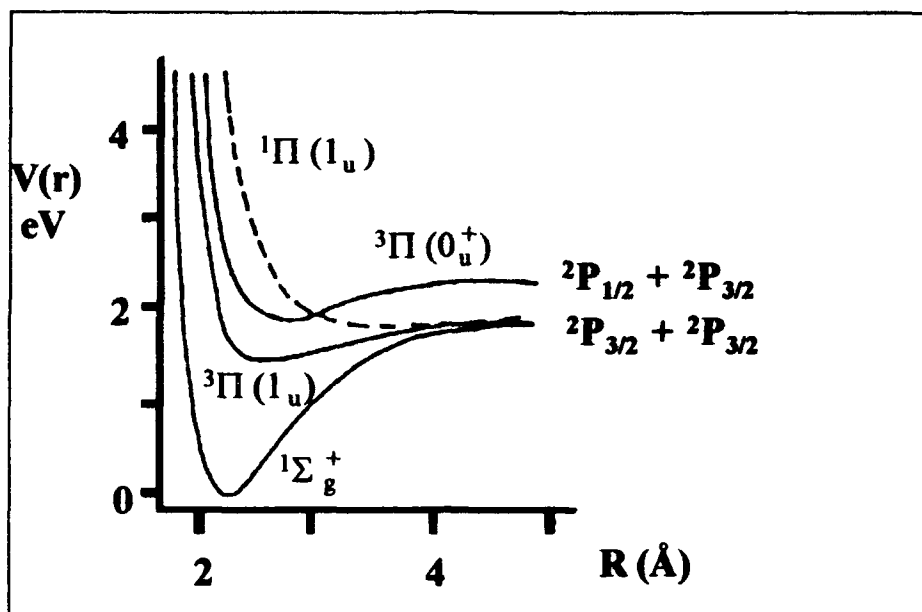


Fig 13: Potential energy curves for molecular bromine ⁽¹⁶⁾

Clearly, excitation of the molecule up to the $1\Pi(1_u)$ state would result in photodissociation, but the products would be two ground state atoms. The $3\Pi(0_u^+)$ state is weakly bound. If this state could be accessed above the dissociation limit, the result would be one excited atom and one ground state atom.

APPENDIX B: TRANSMISSION OF COLD NO FILTER

This section contains plots of the transmission of the cold NO filter. The plots were made with the FTIR, at 0.02 cm^{-1} resolution. The first plot shows a the transmission over the entire range between the cutoff of the interference filter and the cutoff of the detector. For more detail, a section of this is expanded and shown in figure 15.

Note the clear rotational distribution of the 1-0 transition. The minima of the transmission appear to be split, which is a result of two nearly degenerate electronic states acting as a sort of dual ground state. The two states are split by about a hundred wavenumbers, but the vibrational and rotational constants are such that the transitions are almost degenerate. This agrees with the transitions predicted using the published values of the constants to the Dunham expansion.^(14,15) The same set of constants was used to predict the rotational distribution of the 2-1 transition when finding the overlap of the two spectra as discussed in Chapter 3.

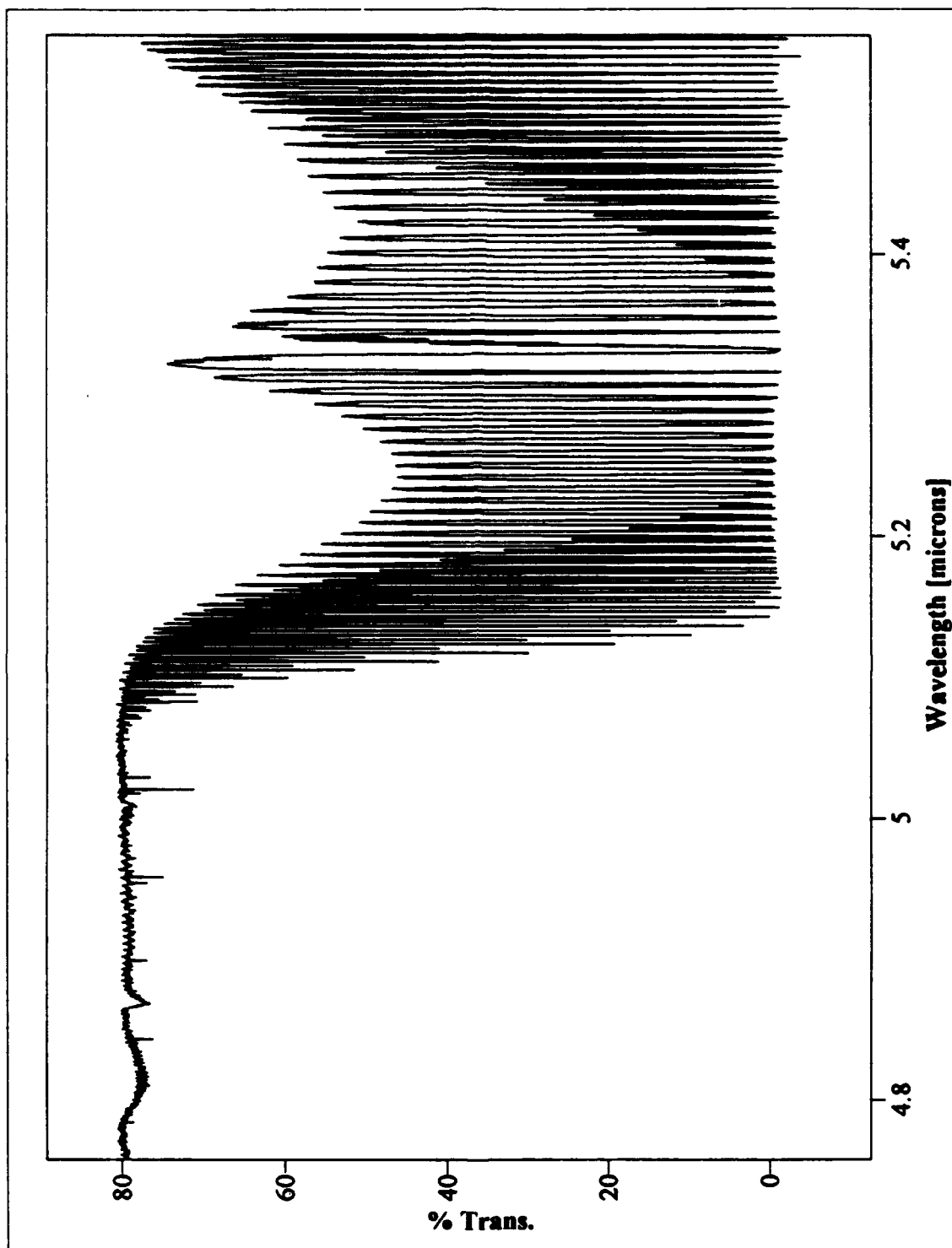


Fig 14: Transmission of cold NO filter, from FTIR

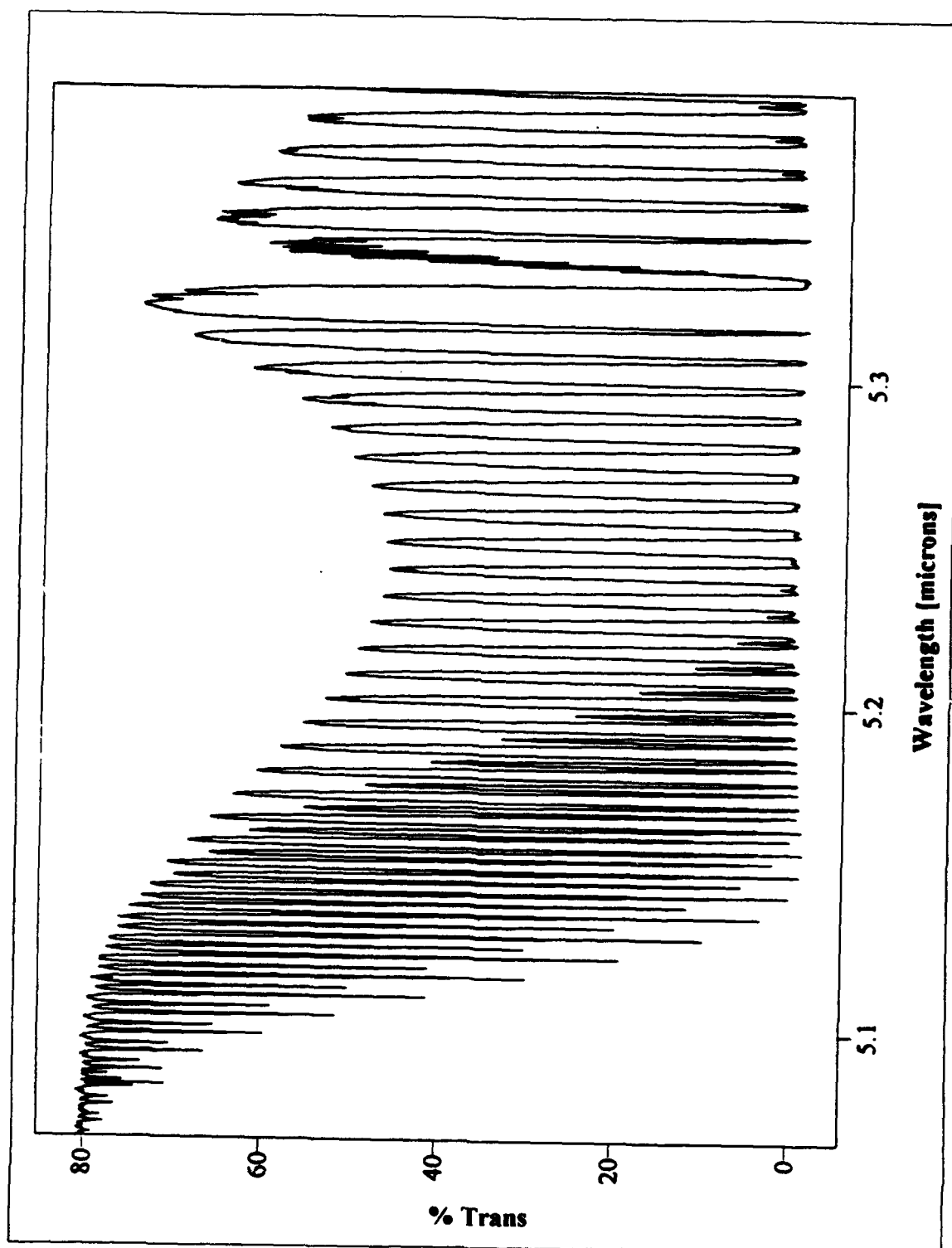


Fig 15: Detail of cold NO filter transmission (0.02 cm^{-1} resolution)

APPENDIX C: FLUORESCENCE DATA FOR NO

This section contains all observations of NO fluorescence. In figures 16 through 19, the observed fluorescence with and without the cold filter are compared for various values of bromine concentration. In most of these charts, the data taken with the cold filter in place has been magnified by some arbitrary scalar in order to show detail. Figure 20 shows a comparison of all of the data taken with the cold NO filter in place, while figure 21 compares all of the data taken without the cold filter.

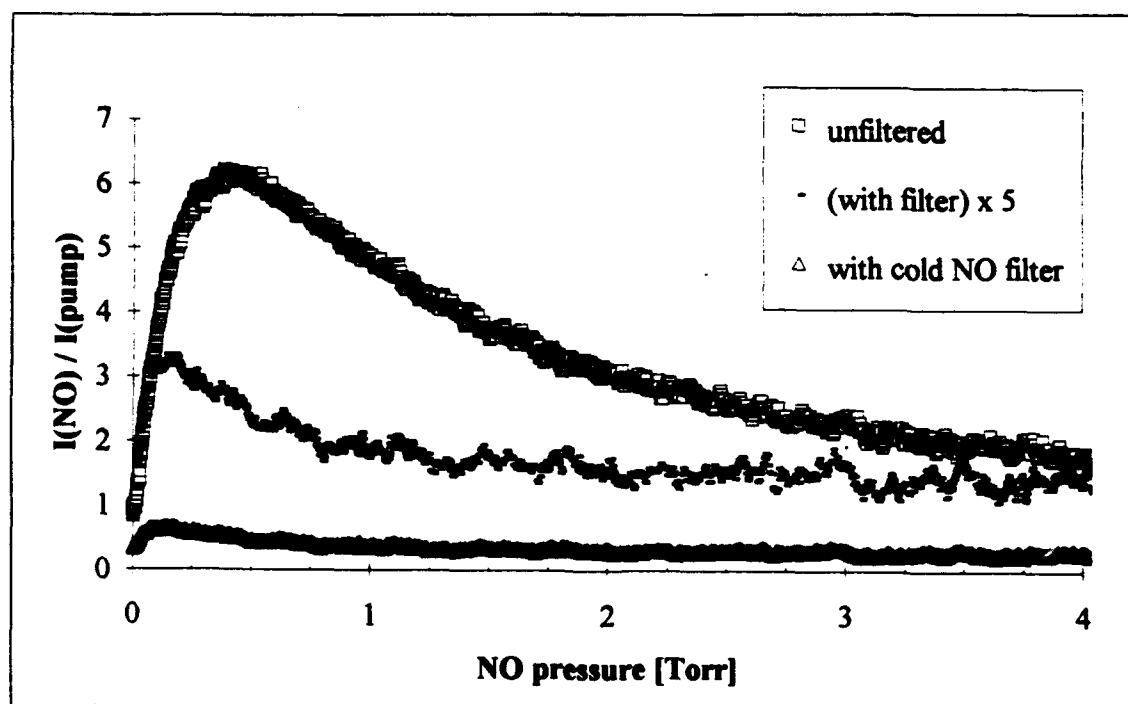


Fig 16: NO fluorescence vs. NO pressure with 500 mTorr of bromine, with and without cold filter.

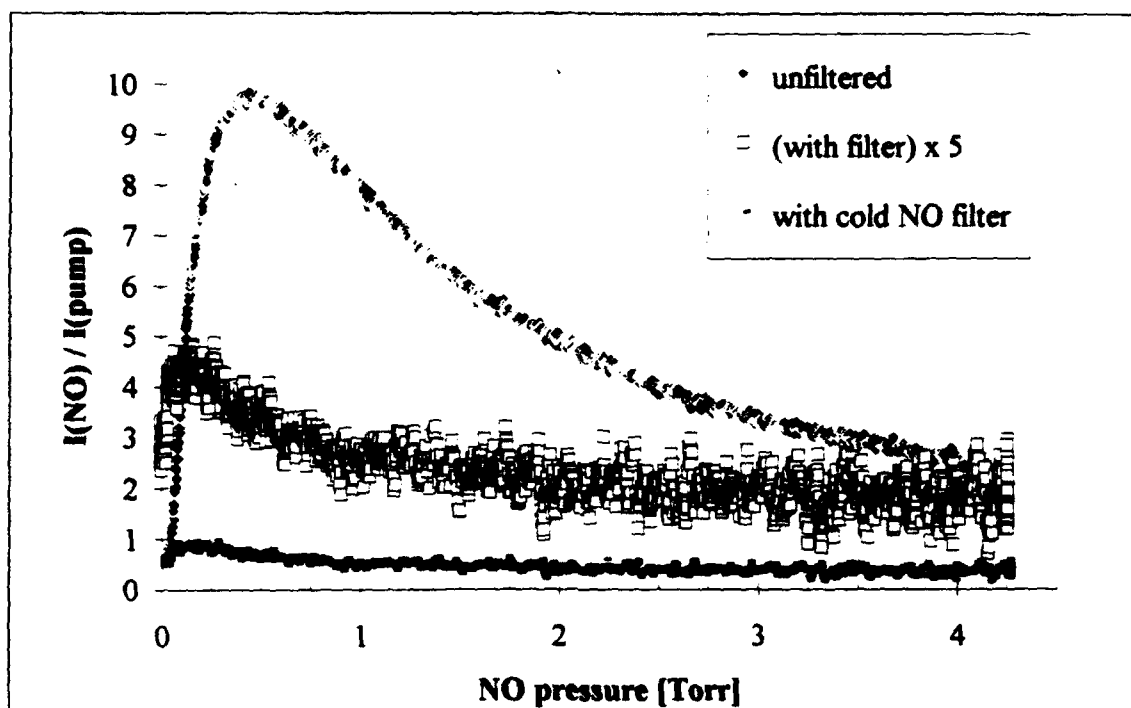


Fig 17: NO fluorescence vs NO press with 750 mTorr of bromine, with and without cold filter. Squares show filtered data multiplied by 5 to show detail.

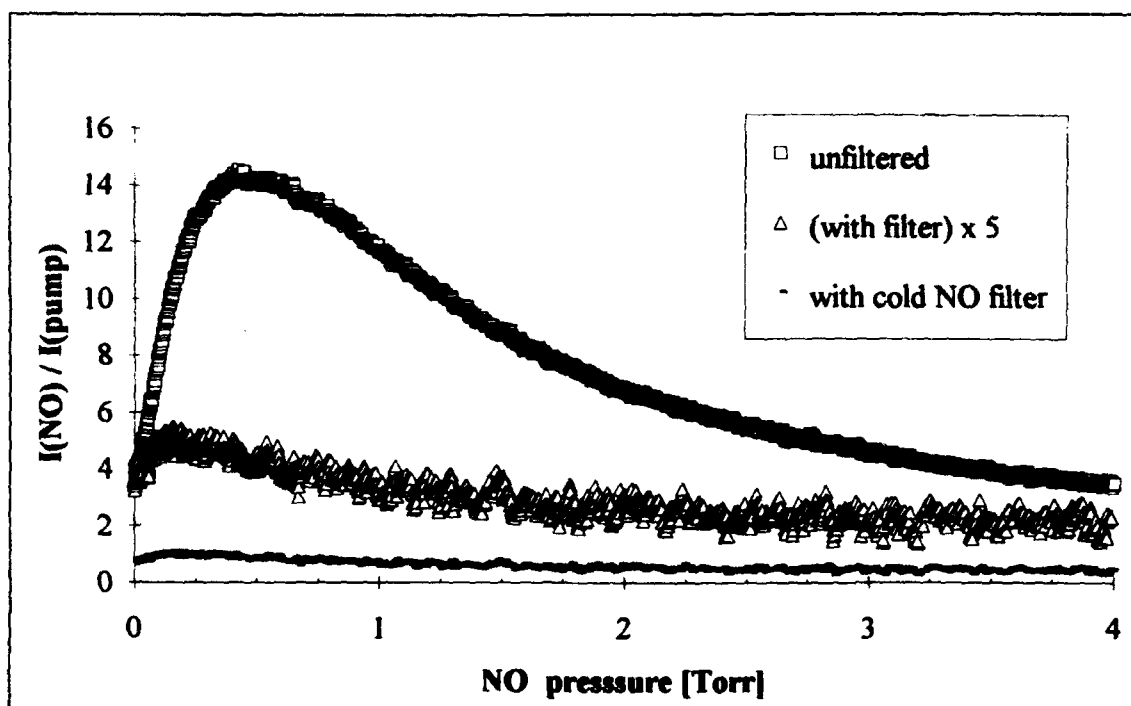


Fig 18: NO fluorescence vs NO pressure for 1.0 Torr bromine, with and without cold filter.

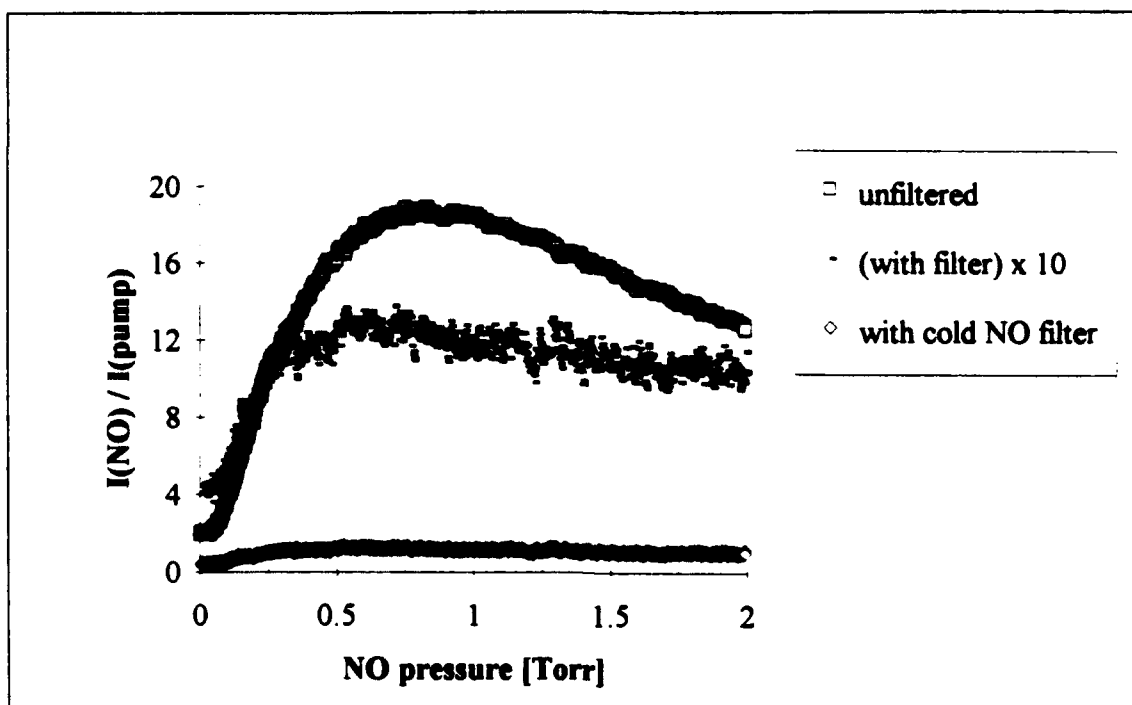


Fig 19: NO fluorescence vs NO pressure for 3.0 Torr bromine, with and without cold filter.

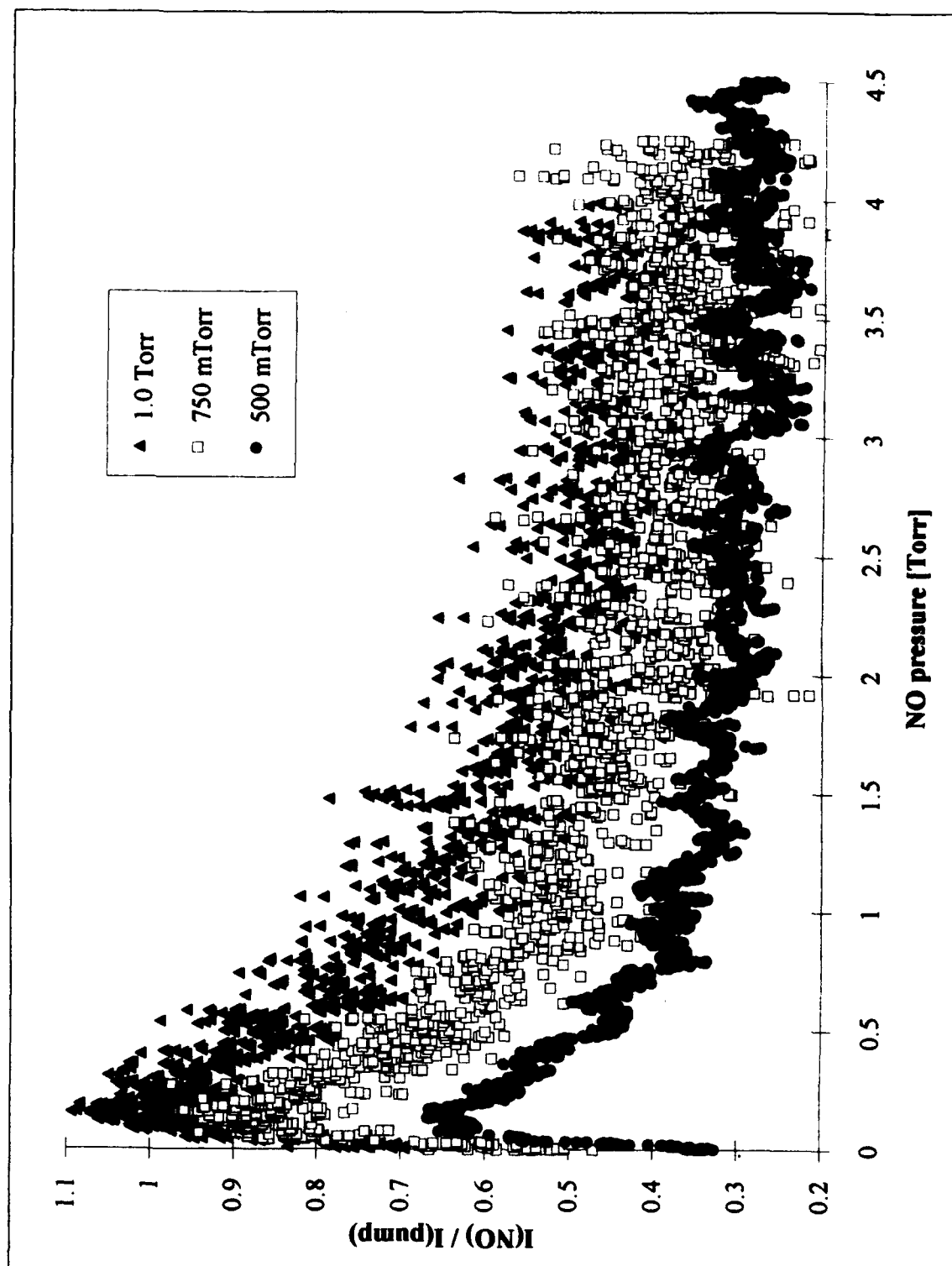


Fig 20: NO fluorescence vs NO pressure with cold filter, for a family of bromine pressures.

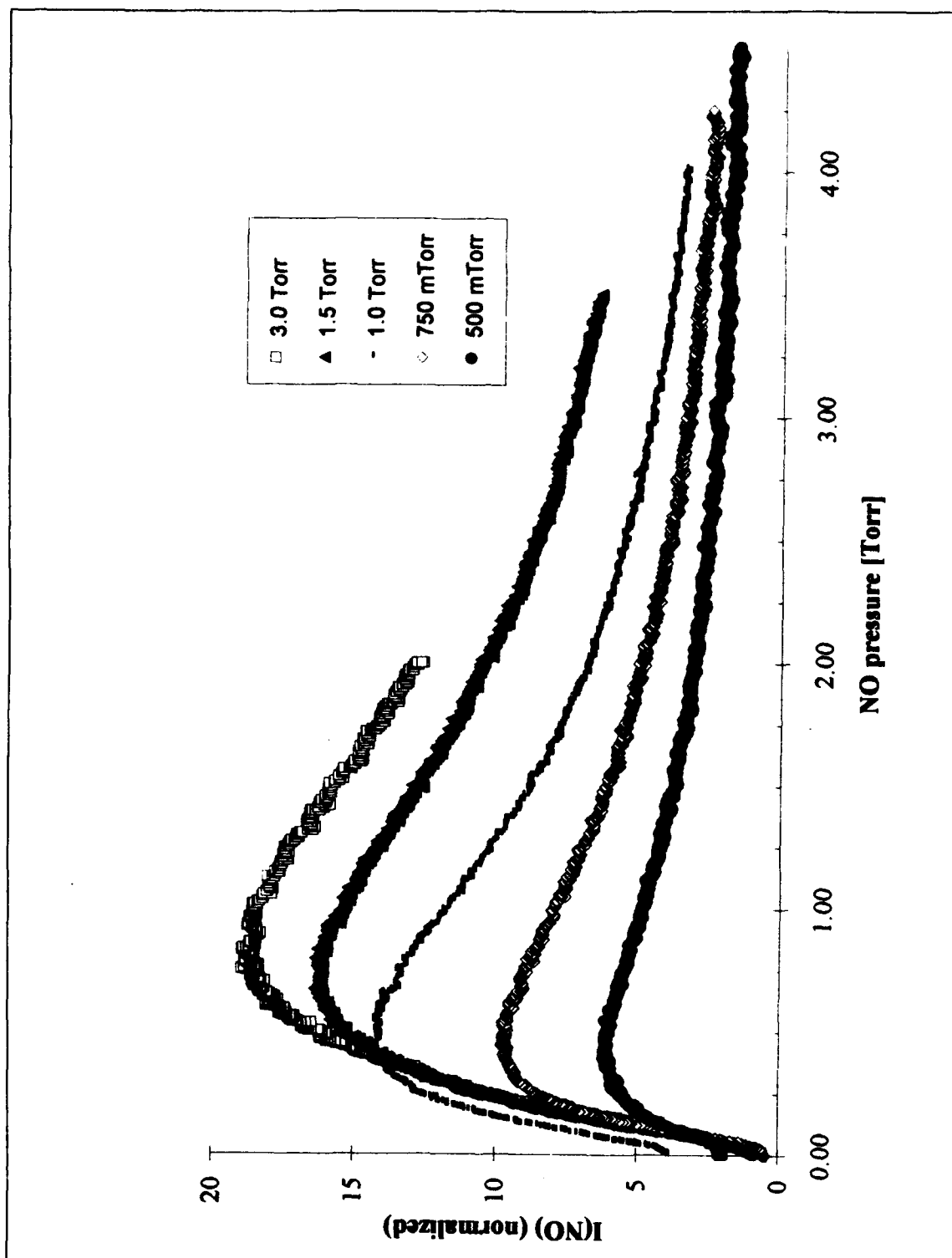


Fig 21: NO fluorescence vs NO pressure, viewed without cold filter, for a family of bromine pressures.

APPENDIX D: ANALYSIS OF FUNCTIONAL FORM USED IN CURVE-FITTING

This section outlines the development of the functional form used to interpolate the data for the observed fluorescence with the cold NO filter in place.

From equation 9, the fluorescence intensity from NO observed through the filter is

$$I_{NO}^{(c.f.)} = D_{5,4}^{(c.f.)} A_{21} [NO(2)] + D_{5,3}^{(c.f.)} A_{10} [NO(1)]$$

From the transmission of the cold NO filter (Fig. 15), it is clear that all of the $1 \rightarrow 0$ transition is blocked, so $D_{5,3}^{(c.f.)} = 0$. This leaves

$$I_{NO}^{(c.f.)} = D_{5,4}^{(c.f.)} A_{21} [NO(2)]$$

By substituting the populations for NO(2) from equation 3c, the result is

$$I_{NO}^{(c.f.)} = \frac{D_{5,4}^{(c.f.)} A_{21} k_2 [NO(0)] [Br^*]}{\Gamma_2 + k_Q^{(2)} [Br_2] + k_{V-T}^{(2)} [NO(0)] + k_{V-V} [NO(0)]}$$

And using the Br^* population from equation 3a, the intensity can be written as

$$I_{NO}^{(c.f.)} = \frac{D_{5.4}^{(c.f.)} A_{21} k_2 k_{\text{pump}} I_{\text{pump}} [NO(0)] [Br_2]}{a [NO(0)]^2 + b [NO(0)] + c}$$

where $a = (k_{V-T}^{(2)} + k_{V-V})(k_1 + k_2)$

$$b = (k_{V-T}^{(2)} + k_{V-V})(\Gamma_{Br} + k_Q^{(Br)} [Br_2]) \\ + (k_1 + k_2)(\Gamma_2 + k_Q^{(2)} [Br_2])$$

$$c = (\Gamma_2 + k_Q^{(2)} [Br_2])(\Gamma_{Br} + k_Q^{(Br)} [Br_2])$$

By dividing top and bottom of this equation by c and factoring the denominator, this can be recast in the form

$$I_{NO}^{(c.f.)} = \frac{\alpha [NO(0)]}{(\beta [NO(0)] + 1)(\gamma [NO(0)] + 1)}$$

where $\alpha = \frac{D_{5.4}^{(c.f.)} A_{21} k_2 k_{\text{pump}} I_{\text{pump}}}{(\Gamma_2 + k_Q^{(2)} [Br_2])(\Gamma_{Br} + k_Q^{(Br)} [Br_2])}$

$$\beta = \frac{(k_{V-T}^{(2)} + k_{V-V})}{(\Gamma_2 + k_Q^{(2)} [Br_2])}$$

$$\gamma = \frac{(k_1 + k_2)}{(\Gamma_{Br} + k_Q^{(Br)} [Br_2])}$$

Which, of course, is the form used for the curve-fitting.

VITA

Michael R. Hawks was born in Lansing, Michigan on 3 August, 1969, and grew up near Potterville, Michigan; a thriving metropolis with a triple digit population. He went to college at Michigan State University, where he received a B.S. in Astrophysics, with a minor in Renaissance art. While at MSU, he was a member of AFROTC, and served as Director of Public Affairs on the Area IX HQ staff of Arnold Air Society. Upon graduating in June of 1991, he was commissioned into the Air Force, but did not come on active duty until reporting to AFIT in scenic Dayton, Ohio, nearly one year later. Upon graduation from AFIT, he will go to Phillips Lab, at Kirtland AFB to work in the Active Imaging Branch. While at Kirtland, he hopes to finally return to his favorite hobbies: golf and entropy.

Permanent Address:

6429 Hartel Rd.

Potterville, MI 48876

REPORT DOCUMENTATION PAGE			Form Approved OMB No. 0704-0188	
<small>Public reporting burden for this collection of information is estimated to average 1 hour per response, including the time for reviewing instructions, searching existing data sources, gathering and maintaining the data needed, and completing and reviewing the collection of information. Send comments regarding this burden estimate or any other aspect of this collection of information, including suggestions for reducing this burden, to Washington Headquarters Services, Directorate for Information Operations and Reports, 1215 Jefferson Davis Highway, Suite 1204, Arlington, VA 22202-4302, and to the Office of Management and Budget, Paperwork Reduction Project (0704-0188), Washington, DC 20503.</small>				
1. AGENCY USE ONLY (Leave blank)		2. REPORT DATE December 1993		3. REPORT TYPE AND DATES COVERED Master's Thesis
4. TITLE AND SUBTITLE Infrared Fluorescence Studies of Electronic-to-Vibrational Energy Transfer in a Br ₂ :NO System.				5. FUNDING NUMBERS
6. AUTHOR(S) Michael R. Hawks, First Lieutenant, USAF				
7. PERFORMING ORGANIZATION NAME(S) AND ADDRESS(ES) Air Force Institute of Technology, WPAFB OH 45433-6583				8. PERFORMING ORGANIZATION REPORT NUMBER AFIT/GAP/ENP/93D-03
9. SPONSORING/MONITORING AGENCY NAME(S) AND ADDRESS(ES) Dr. E. Dorko PL/LID 3550 Aberdeen SE Kirtland AFB, NM 87117-5776				10. SPONSORING/MONITORING AGENCY REPORT NUMBER
11. SUPPLEMENTARY NOTES				
12a. DISTRIBUTION AVAILABILITY STATEMENT Approved for public release; distribution unlimited				12b. DISTRIBUTION CODE
13. ABSTRACT (Maximum 200 words) <p>Steady-state photolysis techniques were used to study electronic-to-vibrational energy transfer mechanisms from atomic bromine to nitric oxide. Molecular bromine was photodissociated by 488nm radiation to produce equal parts Br(2P_{1/2}) and Br(2P_{3/2}). Side fluorescence intensity from Br(2P_{1/2}) at 2.7 microns and from NO(v=1 and 2 around 5.3 microns were measured as a function of bromine pressure and nitric oxide pressure. The branching ratio for collisional transfer into the first and second excited states of NO was determined, and previously reported rates for quenching of NO by molecular bromine were verified.</p>				
14. SUBJECT TERMS nitric oxide, bromine, E-V transfer, infrared fluorescence, photolysis				15. NUMBER OF PAGES 68
				16. PRICE CODE
17. SECURITY CLASSIFICATION OF REPORT Unclassified	18. SECURITY CLASSIFICATION OF THIS PAGE Unclassified	19. SECURITY CLASSIFICATION OF ABSTRACT Unclassified	20. LIMITATION OF ABSTRACT UL	